Supplementary Appendix

This appendix has been provided by the authors to give readers additional information about their work.

Supplement to: Zhou Q, Yang D, Ombrello AK, et al. Early-onset stroke and vasculopathy associated with mutations in ADA2. N Engl J Med 2014;370:911-920. DOI: 10.1056/NEJMoa1307361

TABLE OF CONTENTS

AUTHORS' CONTRIBUTIONS

Qing Zhou, Daniel L. Kastner, and Ivona Aksentijevich designed the study.

Qing Zhou, Dan Yang, Amanda K. Ombrello, Camilo Toro, Deborah L. Stone, Sergio D. Rosenzweig, Kevin Bishop, Karyl Barron, Hye Sun Kuehn, Patrycja Hoffmann, Alejandra Negro, Wanxia L. Tsai, Edward W. Cowen, Wuhong Pei, Joshua D. Milner, Christopher Silvin, Theo Heller, David T. Chin, Nicholas J. Patronas, John S. Barber, Chyi-Chia R. Lee, Geryl M. Wood, Alexander Ling, Susan J. Kelly, David E. Kleiner, Nancy J. Ganson, Heidi H. Kong, Sophie Hambleton, Martha M. Quezado, Katherine Calvo, Hawwa Alao, Beverly K. Barham, Anne Jones, James F. Meschia, Bradford B. Worrall, Scott E. Kasner, Stephen S. Rich, Raphaela Goldbach-Mansky, Mario Abinun, Elizabeth Chalom, Alisa C. Gotte, Marilynn Punaro, Virginia Pascual, James Verbsky, Troy R. Torgerson, Nora G. Singer, Timothy R. Gershon, Seza Ozen, Omer Karadag, Elaine F. Remmers, Raman Sood, and Ivona Aksentijevich gathered the data.

Qing Zhou, Andrey V. Zavialov, Anton V. Zavialov, Jae Jin Chae, Joshua D. Milner, James Mullikin, Fabio Candotti, Thomas A. Fleisher, Shawn M. Burgess, Susan L. Moir, Massimo Gadina, Raman Sood, Michael Hershfield, Manfred Boehm, and Ivona Aksentijevich analyzed the data.

All authors vouch for the data and the analysis.

Qing Zhou, Elaine F. Remmers, Daniel L. Kastner, and Ivona Aksentijevich wrote the paper.

All authors agreed to publish the paper.

SUPPLEMENTARY METHODS

Exome sequencing

Genomic DNA samples for exome sequencing were prepared from peripheral blood using the Maxwell® 16 Blood DNA Purification Kit (Promega). Exome sequence libraries were prepared using an Illumina TruSeq DNA Sample Preparation Kit version 2. Paired-end sequencing was performed on the Illumina HiSeq2000 instrument. BWA software was used to align the sequence reads to the Human Reference Genome Build hg19. Picard was used to identify PCR duplicates. GATK was used to realign the sequence reads around microindels to produce a better alignment and to recalibrate the base qualities to obtain more accurate quality scores. GATK Unified Genotyper (parameters: -stand_call_conf 5.0, -stand_emit_conf 5.0, -dcov 500) and SAMtools were then used to identify SNVs and Indels. ANNOVAR was used for annotation.

Sanger sequencing

Coding exons of *CECR1* were sequenced using the BigDye Terminator v1.1 Cycle Sequencing kit (Applied Biosystems) following the manufacturer's instructions. Sequencing was performed on a 3130xl Genetic Analyzer (Applied Biosystems). Sequencing data were analyzed using Sequencher (Gene Codes).

High density SNP bead chip array and single base extension genotyping

A high density SNP bead chip array (HumanOmniExpress, Illumina) was used for detecting the large genomic deletion. The HumanOmniExpress data were

analyzed by Nexus Copy Number software (BioDiscovery, Hawthorne, California) using annotations of genome version hg19.

A total of 1131 Turkish healthy control samples were genotyped for the p.Gly47Arg variant using the Sequenom iPLEX gold method (Sequenom, San Diego, California). Genotypes were determined using Typer 4.0 software (Sequenom).

Controls used for functional and genetic studies

We used healthy controls for various functional assays. Written informed consent was obtained from all participants. We used 6 Caucasian pediatric healthy controls of age less than 13y and 11 Caucasian adult controls to assay the ADA2 activity in serum. The same controls were used in B cell and T cell assays. For measuring ADA1 enzymatic activity in hemolysates and in human monocytes, we utilized a set of adult healthy controls used in the reference laboratories. We used 1131 Turkish healthy controls for determining the frequency of the p.Gly47Arg variant in the Turkish population.

Enzyme-linked immunosorbant assay (ELISA) for measurement of ADA2 activity in plasma and serum

ELISA plates (Perkin Elmer) were coated overnight at 4°C with 100 µl of 5 µg/ml anti-ADA2 polyclonal antibodies.[1] After washing the plates with PBS-Tween20 and blocking with 2% BSA in PBS, 100 µl of recombinant ADA2 standards or serum or plasma samples diluted in complete RPMI medium were added to the

wells, and the plates were incubated for 4 hours at RT. Subsequently, the plates were washed with PBS-Tween20 and 100 µl of 2 mM adenosine in 0.1M Tris-HCl pH 6.8 was added. The plate was incubated at 37°C for 18 hours. The reaction was stopped by transferring 10 µl of the reaction mix into a UV-transparent plate (Corning) containing 190 µl of water per well. The ratio of absorbance at 265 and 245 nm was detected on a Synergy H1 hybrid Reader (Biotek) and the ADA2 activity in the samples was determined from a standard curve generated with wild type recombinant protein. (Figure 2A)

Measurements of ADA1 and ADA2 activity in plasma

An HPLC method for accurate measurement of both ADA1 and ADA2 was developed by SJ Kelly, NJ Ganson, and MS Hershfield (unpublished). Briefly, assays were performed in 100 µL (total volume) containing 100 mM potassium phosphate, pH 7.0, 10 µL of undiluted plasma, and either no inhibitor or 100 µM of the selective ADA1 inhibitor, erythro-9-(2-hydroxy-3-nonyl) adenine (EHNA, Sigma). After 5 min (at 37°C), the assay was initiated by adding adenosine to a final concentration of 10 mM. After 30 min and 120 min of incubation, 44 µL of the assay was removed, mixed with 11 µL of 5N perchloric acid, and placed on ice. After centrifugation for 2 min at 20,000 x g, 40 µL of supernatant was removed and neutralized with 11 µL of 3N KOH, 1M $KHCO_3$. After centrifugation as above, 30 µL of neutralized supernatant was analyzed by HPLC on a Waters Corporation C18 µBondapak column (3.9 x 300 mm), using a mobile phase of 0.05 M $(NH_4)H_2PO_4$, 8% methanol, 1% acetonitrile, pH 5.2 (flow rate 1 mL per

min), and using a diode array detector and monitoring absorbance at 260 and 280 nm. Both inosine and hypoxanthine were quantified, to account for the inosine converted to hypoxanthine during the reaction, presumably by the action of purine nucleoside phosphorylase present in plasma in variable amounts. After calculation of total ADA activity (inosine plus hypoxanthine formed in the absence of EHNA), and ADA2 activity (inosine plus hypoxanthine formed in the presence of EHNA), ADA1 activity was calculated by subtracting ADA2 from total ADA activity. All ADA activity was expressed as nmoles of inosine + hypoxanthine formed per min per mL of undiluted plasma (mU mL^{-1} plasma). (Table S7)

ADA1 and ADA2 enzymatic activity assay in $CD14^+$ monocytes

PBMCs were isolated from peripheral blood of healthy controls or patients by Ficoll separation (MP Biomedicals) according to the manufacturer's specifications. $CD14^+$ monocytes were purified from PBMCs using a DynabeadFlowComp Human CD14 isolation kit (Invitrogen). Purity of 97-100% was obtained as evaluated by staining cells with phycoerythrin (PE)-labeled mouse monoclonal anti-Human CD14 antibody (Invitrogen) and FACS analysis (FACSCanto, BD Biosciences).

ADA assays were performed as described[2] with some modifications. Briefly, 5×10^5 purified monocytes or PBMCs were lysed in 100 μL M-Per (Pierce) at room temperature. After centrifugation, 10 μL 1 mM ^{14}C-adenosine (Moravek) was added to 10 μL cell lysate and incubated for 10 to 40 minutes at 37°C in the absence or presence of 33uM EHNA. The reaction was stopped by

heating to 95°C for 5 minutes and samples were transferred to ice. The reaction mixture (4-10 μL) was spotted onto thin-layer chromatography (TLC) plates (Analtech) previously loaded with 3 uL 0.1 M standards of unlabeled adenosine, hypoxanthine, and inosine (all from Sigma) and dried. Separation was obtained by placing TLC plates in a solution of 0.1 M sodium biphosphate, pH 6.8 (10 parts), 6 parts saturated ammonium sulfate, and 0.2 parts n-propyl alcohol for 120-140 minutes. Plates were dried and exposed to a phosphoimager screen for 36 to 40 hours. Pixels were counted with a FujiFilm BAS 1500 Phosphoimager. ADA units were determined as nanomoles adenosine deaminated per minute per 10^8 cells. The healthy control mean and normal range for ADA1 and ADA2 activities were determined in monocyte lysates from 12 healthy blood donors. (Figure S10A, B)

Thin-layer chromatographic assay for ADA1 activity in erythrocyte hemolysates (Figure S10C) and **HPLC assay for deoxyadenosine and adenosine nucleotides** (Figure S10D) were performed as previously described.[3,4]

Immunoblotting mononuclear cell lysates and supernatants

Peripheral blood mononuclear cells (PBMCs) were isolated by LSM-Lymphocyte Separation Medium (50494, MP Biomedicals) from freshly drawn peripheral venous blood from healthy controls or patients. Isolated PBMCs were used directly or were differentiated into macrophages with 800 units/ml of GM-CSF

(Peprotech). PBMCs or macrophages (2.0×10^6 cells per well) were plated in 12-well plates and then primed with RPMI 1640 containing 10% FBS, antibiotics, and 1 μg ml^{-1} LPS for 3 hours. The medium was replaced with RPMI 1640 medium. After 1 hr, supernatants and cell lysates were collected and subjected to SDS-PAGE for Western blot analysis using primary antibodies (Abs); anti-human ADA2 Ab previously described,[1] and anti-human actin Ab (Santa Cruz Biotechnology).

Whole blood cell stimulation and cytokine assays

Whole blood samples from patients or healthy controls were collected in sodium heparin tubes. The whole blood was washed with PBS (Life Technologies) three times at 2000 × g for 10 min at room temperature. The whole blood cell pellets were then resuspended in RPMI1640 medium (Life Technologies), and the numbers of whole blood cells were counted. The washed whole blood cells, 2×10^6 cells per ml, were plated into a well of a 48-well plate. The whole blood cells were left untreated or stimulated with the following stimuli (InvivoGen): Pam_3CSK_4, lipopolysaccharide (LPS), and Staphylococcal Enterotoxin B (SEB) at 1μg/ml; Poly(I:C), zymosan, and muramyldipeptide (MDP) at 10μg/ml; flagellin at 50 ng/ml; FSL1 (Pam_2CGDPKHPKSF) at 100 ng/ml; imiquimod at 5μg/ml; ssRNA at 0.25μg/ml; heat-killed *Listeria monocytogenes* (HKLM) at 10^7 bacteria/ml; and ODN2006 at 5 μM. Whole blood cells were incubated at 37°C, 5% CO_2 for 24 hrs. After centrifugation, the supernatants of the whole blood cell culture were collected and stored at -80° C for cytokine immunoassay.

The concentrations of 48 cytokines were detected using the Bio-Plex pro human cytokine 27-plex and 21-plex immunoassays (Bio-Rad) according to the manufacturer's instructions. Human cytokine standards group I and II were used for the standard curves. 50 µl of whole blood cell culture supernatants or serum samples (after a 1:1 dilution with Bio-Plex sample diluent for the sera) were used for the immunoassays. The data were plotted and analyzed for significance using the Mann-Whitney test ($P< 0.05$). The 48 cytokines and growth factors assayed are: IL-1α, IL-2Rα, IL-3, IL-12 (p40), IL-16, IL-18, CTACK, GRO-α, HGF, IFN-α2, LIF, MCP-3, M-CSF, MIF, MIG, β-NGF, SCF, SCGF-β, SDF-1α, TNF-β, TRAIL, IL-1β, IL-1ra, IL-2, IL-4, IL-5, IL-6, IL-7, IL-8, IL-9, IL-10, IL-12 (p70), IL-13, IL-15, IL-17, basic FGF, eotaxin, G-CSF, GM-CSF, IFN-γ, IP-10, MCP-1 (MCAF), MIP-1α, MIP-1β, PDGF-BB, RANTES, TNF-α, VEGF.

Flow cytometry and analysis of U937 cell differentiation

The following surface and intracellular markers were used for T cell assays: Aqua viability dye and CD3-Qdot605 (both Invitrogen), CD4-PE-Cy7, CD8-APC-H7, CD45RO-TRPE, CD27-PE-Cy5, CD69-FITC, CD98-PE, IL-2-FITC, and IFN-γ-AF700 (all BD Biosciences). The Foxp3 staining kit and protocol (eBioscience) were used to stain for intracellular cytokines. All T cell experiments were gated on live, $CD3^+$, singlets. For the U937 cell flow cytometry assay, scrambled control shRNA-transduced, or *CECR1* (ADA2) shRNA-transduced U937 cells were seeded in 12-well plates (1,000,000 cells/well). Cells were differentiated to macrophages by PMA (20 ng/ml) treatment for 5 days. Adherent and non-

adherent cells were collected for flow cytometry. After fixing with 4% paraformaldehyde for 10 min and washing with PBS, cells were suspended in 0.1% saponin/PBS buffer for 15 min, followed by allophycocyanin (APC)–conjugated anti-CD68 (Biolegend) staining for 30 min on ice. After washing with 0.1% saponin/PBS buffer, cells were analyzed using a FACS Canton II (BD Biosciences).

T cell activation assay

PBMCs were stimulated overnight in X-Vivo15 media (Lonza) with anti-CD3 (OKT3, 1 µg/ml, eBioscience) and stained for phenotypic and activation markers. $CD4^+$ or $CD8^+$ cells were gated on naïve ($CD45RO^-CD27^+$) or memory ($CD45RO^+CD27^+$, $CD45RO^+CD27^-$ and $CD45RO^-CD27^-$) and analyzed for CD69 and CD98.

T cell proliferation assay

PBMCs were stained with carboxyfluorescein diacetate succinimidyl ester (CFSE, CellTrace CFSE Proliferation Kit, Invitrogen) and stimulated for five days in X-Vivo15 media with anti-CD3 (OKT3, 1 ug/ml) or PHA (6.25 ug/ml, Thermo) and $CD4^+$ or $CD8^+$ cells analyzed for CSFE dilution.

T cell cytokine assay

Ex vivo PBMCs were stimulated overnight with PMA (20 ng/ml) and ionomycin (1 uM) (both Calbiochem) in the presence of Brefeldin A (10 ug/ml, Sigma), in X-

Vivo15 media. $CD4^+$ or $CD8^+$ cells were gated on memory ($CD45RO^+CD27^+$, $CD45RO^+CD27^-$ and $CD45RO^-CD27^-$) and analyzed for IFN-γ and IL-2 production.

B cell death/apoptosis

Total freshly isolated PBMCs were cultured in 10% FBS/RPMI for 48 hours and stained with anti-CD19 (B cells) and propidium iodide (PI) to identify dead B cells (those that cannot exclude the dye), and apoptotic cells (those with fragmented DNA and therefore intermediate intensity PI staining). After 20 minutes, cells were analyzed by flow cytometry (FACSCanto II, BD Biosciences).

B cell immunophenotyping and functional assays

Peripheral blood mononuclear cells (PBMC) were isolated from whole blood by density gradient centrifugation (Hypaque-Ficoll). PBMCs were stained with the following mAb-fluorochrome combinations: CD10-APC, CD19-PerCP-Cy5.5 and CD20-APC-H7 from BD Biosciences; CD27-PE-Cy7 from eBioscience and CD21-FITC from Beckman Coulter. The capacity of PBMC B cells to proliferate in response to B cell stimuli and express markers of memory was assessed by CFSE dilution as previously described.[5] Additional mAb-fluorochrome combinations for CFSE analyses included IgG-PE from BD Biosciences and CD3-V510 from Biolegend. The capacity of PBMC B cells to terminally differentiate and secrete immunoglobulin (Ig) was assessed by ELISPOT as previously described,[6] with the following specifications. PBMCs were stimulated

for five days, after which a portion was used for ELISPOT and another portion was immunophenotyped in order to calculate frequencies of Ig-secreting cells per million B cells.

Zebrafish studies

Zebrafish (*Danio rerio*) were maintained at the National Human Genome Research Institute (NHGRI) under Animal Care and Use Committee-approved protocols. All zebrafish handling and breeding was performed using established methods from The Zebrafish Book[7]. Knockdown of the *CECR1* zebrafish paralog, *cecr1b,* was performed by morpholino injection.

Zebrafish morpholino studies

Two *cecr1b*-specific antisense morpholinos were obtained from Gene Tools. Both morpholinos were tagged at the 3' end with fluorescein to allow identification of injected embryos. Microinjections were performed into the yolk sac at the 1-cell to 4-cell stage. Embryos were raised at 28°C and scored for survival and development at 24 hours post fertilization (hpf). Embryos were then incubated with phenylthiourea in Embryo Medium (E3) to suppress pigmentation and observed for EGFP and DsRed expression using a Zeiss fluorescent Axiophot microscope or fixed for whole mount *in situ* hybridizations (WISH) and o-dianisidine staining at 48 and 72 hpf[8,9]. To visualize vascular development, *fli1*:EGFP/*gata1*:DsRed[10,11] transgenic fish were studied. To visualize granulocyte development, *mpx*:EGFP[12] transgenic fish were studied.

cecr1b ATG-MO sequence: GCTTATGCTACTCATTGCTCCCAGC

cecr1b E3I3-MO sequence: TAACTTTGATGTTCGCTCACCTGTT

Zebrafish embryo microscopy

Confocal images were acquired at room temperature using a Zeiss LSM 510 NLO Meta system (Thornwood, NY, USA) mounted on a Zeiss Axiovert 200M microscope with a Plan-Apochromat 10X/0.45 objective lens. Excitation wavelengths of 488nm (3.5%) and 561nm (7.5%) were used for detection of the EGFP and DsRed, respectively. Fluorescent emissions were collected with a BP 500-550nm IR blocked filter and BP 575-615nm IR blocked filter, respectively. Pinhole was set to 1.5 Airy units (AU), which corresponds to an optical slice of 1.1 µm. A range of 36-74 z-slices was used depending on the zebrafish orientation with a 3.0 µm interval. All confocal images were of frame size 512 pixels by 512 pixels, scan zoom of 1.3 to 1.7 and line-averaged 4 times. Images were collected using the Zeiss ZEN 2009 V5.5 SP2 software package. Z-stacks were then processed using Bitplane's Imaris x64 3D software program version 7.5.2 (Zurich, Switzerland). Volume renderings were made using either maximum projection or normal shading options.

Immunofluorescence staining of shRNA-transduced U937 cells

Scrambled control shRNA-transduced, or *CECR1* (ADA2) shRNA-transduced U937 cells were seeded in 12-well plates (1,000,000 cells/well). Cells were differentiated to macrophages by PMA (20 ng/ml) treatment for 5 days. All

adherent and non-adherent cells were collected, mixed, and cytospun onto glass slides. After fixing with 4% paraformaldehyde for 10 min and washing with PBS, blocking solution (5% normal donkey serum in PBS with 0.3% Triton-X100) was applied for 1 h. Primary antibody mouse anti-human CD68 (1:50, DAKO) was incubated overnight at 4°C. Cells were washed with PBS, and corresponding secondary antibody was applied for 1 h at RT. Nuclear staining was performed through immersion in DAPI (1:1000, Invitrogen). Cells were imaged using a Nikon Eclipse TE300 inverted fluorescence microscope. Three replicates were performed for every observation.

Tissue immunohistochemistry

Fresh skin biopsy tissues were fixed with 4% paraformaldehyde in phosphate buffered saline (PBS) overnight at 4^{o}C and placed in 20% sucrose for 6 hours, embedded in OCT, frozen, and sectioned. Serial cryosections (6 μm) were cut. For frozen section immunostaining, thawed slides were washed in PBS and blocked using 5% donkey serum in PBS with 0.1% Triton-X100. The following primary antibodies were then applied overnight at 4^{o}C at the specified concentrations: anti-vWF (1:200, DAKO), anti-E-selectin (1:25, R&D), anti-IL-1β (1:100, Abcam), and anti-iNOS (1:100, Abcam). After washing with PBS, appropriate secondary antibodies [donkey Alexa Fluor 488 or 594 labeled (1:1000, Invitrogen)] were applied for 1 h at room temperature (RT). Slides were mounted using DAPI-containing mounting medium (Vector Laboratories).

For staining formalin-fixed, paraffin-embedded skin and brain samples, slides were deparaffinized with two 30 min washes in xylene, followed by two 100% ethanol washes for 1 minute each, and a series of 1 min washes in 90%, 80%, 70%, and 50% ethanol. Slides were then rinsed with water. Antigen retrieval was performed in a solution of 10 mM sodium citrate, pH 6.0 for 40 min at 95°C. After cooling completely, samples were blocked for one hour in 5% BSA, 20% donkey serum in PBS with 0.1% Triton-X100. Primary antibodies for CD31 (1:50, DAKO), iNOS (1:100, Abcam), TNFα (1:100, Abcam), CD68 (1:50, DAKO), MPO (1:200, Abcam), CD3 (1:100, Abcam) and anti-IL-1β (1:100, Abcam) were applied overnight at 4°C, followed by the corresponding secondary antibody [donkey Alexa Fluor 488 or 594 labeled (1:1000, Invitrogen)] for one hour at RT. For brain sample E-selectin staining, 1mM EDTA antigen retrieval solution (pH 8.0) was used and primary E-selectin antibody (1:25, Abcam) and vWF antibody (1:200, DAKO) were incubated for overnight at 4°C. Slides were mounted using DAPI-containing mounting medium. Slides were imaged using a confocal microscope (Zeiss LSM 510 META) at the stated magnifications.

Immunoblotting in HUVECs and HCAECs

HUVECs (Lonza) and HCAECs (Lonza) were cultured in EGM-2 media (Lonza). Cells were initially seeded at 10,000 per cm^2 until confluent. U937 cells (ATCC) were mantained using RPMI 1640 (Gibco) supplemented with 10% FBS, 2 mmol/L L-glutamine, penicillin (100 U/ml), and streptomycin (100 ug/ml). Cells were lysed in RIPA buffer containing protease and phosphatase inhibitors

(Sigma). Recombinant human ADA2 (R&D) was used for positive control. For each sample, 20 µg of total protein was analyzed by Western blot (Biorad 4–20% Mini-PROTEAN® TGX gel). Antibody for ADA2 (1:1000, Sigma) was incubated at 4°C overnight and followed by corresponding secondary antibody for one hour at RT. α-Tubulin was used as loading control.

RNA extraction, reverse transcription and real-time PCR in HUVECs and HCAECs

RNA was isolated from cultured cells using the RNeasy kit (Qiagen) according to the manufacturer's instructions. RNA was quantified using a Nanodrop NP-1000 spectrometer (Wilmington, DE). Reverse transcription was performed using the Taqman kit (Applied Biosystems). Reaction conditions were: 5^{o}C for 10 min, 48^{o}C for 30 min, 95^{o}C for 5 min and 15^{o}C forever. One µg RNA was used per reaction. Subsequently, real-time PCR was performed using the iQ Syber Green kit (Biorad) according to the manufacturer's protocol. 18S RNA served as control. Quantitative PCR conditions were as follows: 95^{o}C for 5 min, with 39 cycles consisting of 95^{o}C for 45 sec, 57^{o}C for 45 sec, 72^{o}C for 45 sec, read at 78^{o}C, and 95^{o}C for 45 sec. Melting curve determination ranged from 72^{o}C to 95^{o}C with 0.2^{o}C increments. RNA expression was analyzed using the $\Delta\Delta$Ct method. qPCR primer sequences (forward and reverse, respectively) : ADA2: ACCATGACGAAGAGTGGTCAG and CCATTCGGATGGATTCTGCG; 18S RNA (control): TTTCGGAACTGAGGCCATGA and GCAAATGCTTTCGCTCTGGTC

Human myeloid cell line U937 cell culture, differentiation, and gene silencing by short hairpin RNA (shRNA) transduction

U937 cells (ATCC) were maintained using RPMI 1640 (Gibco) supplemented with 10% FBS, 2 mmol/L L-glutamine, penicillin (100 U/ml), and streptomycin (100 ug/ml). Human shRNA constructs for *CECR1* (ADA2) and scrambled controls were purchased from Origene and prepared according to manufacturer's protocol. Media containing viral particles was collected 48 and 72 hours after transfection of 293T cells. U937 cells were transduced by incubating with shRNA virus for 48h. Puromycin (2 ug/ml) was added to the medium to generate stable knockdown cell lines. Non-transduced, scramble control-transduced, or *CECR1* (ADA2) shRNA-transduced U937 cells were seeded in 12-well plates (1,000,000 cells/well). Cells were differentiated to macrophages by PMA (20 ng/ml) treatment.

Primary human monocyte differentiation

PBMCs were isolated from whole blood by centrifugation through Ficoll-Paque plus solution (GE healthcare Bio-Sciences AB) and washed twice in PBS. Monocytes were purified from PBMCs by negative selection (Monocyte Isolation Kit II; Miltenyi Biotec). Monocytes were seeded at a density of 150,000/cm^2 and cultured in RPMI 1640 (Gibco) supplemented with 10% FBS, 2 mM L-glutamine, penicillin (100 U/ml), and streptomycin (100 ug/ml). Primary human monocytes were differentiated into macrophages using 50 ng/mL human macrophage colony-stimulating factor (hM-CSF) or 20 ng/ml human granulocyte-macrophage

colony-stimulating factor (hGM-CSF) for 10 days. Media were changed every 2-3 days.

Co-culture of human primary dermal microvascular endothelial cells (hmEC) with U937 myeloid cells and isolated human monocytes

HmEC (Lonza) were maintained in EGM2 growth medium (Lonza). Passage 2-5 cells were used for experiments. Cells (1,000,000/well) were seeded in 12-well fibronectin-coated plates one day before co-culture to form a complete monolayer of endothelial cells. Control shRNA transduced or *CECR1 shRNA* transduced U937 myeloid cells (1,000,000/well) were co-cultured with pre-seeded hmEC for 24 hours. Monocytes were isolated from an ADA2 deficiency patient and a normal control donor and co-cultured with hmEC for 3 days. Cells were fixed with 4% paraformaldehyde for 10 minutes at RT. The primary antibody VE-Cadherin (1:200, Enzo) was applied overnight at 4^{o}C, followed by the corresponding secondary antibody (donkey Alexa Fluor 594 labeled, 1:400) and FITC-conjugated F-actin (1:40, Invitrogen) for one hour at RT. DAPI (1:1000) was used for detection of cell nuclei.

Web Resources

The URLs for data presented herein are as follows:

1000 Genomes Browser, http://browser.1000genomes.org/index.html

dbSNP, http://www.ncbi.nlm.nih.gov/projects/SNP/

NHLBI Exome Sequencing Project (ESP), http://evs.gs.washington.edu/EVS/

PolyPhen-2, http://genetics.bwh.harvard.edu/pph2/

SIFT Genome, http://sift.jcvi.org/

dbGAP, http://www.ncbi.nlm.nih.gov/gap

SUPPLEMENTARY FIGURES

Figure S1

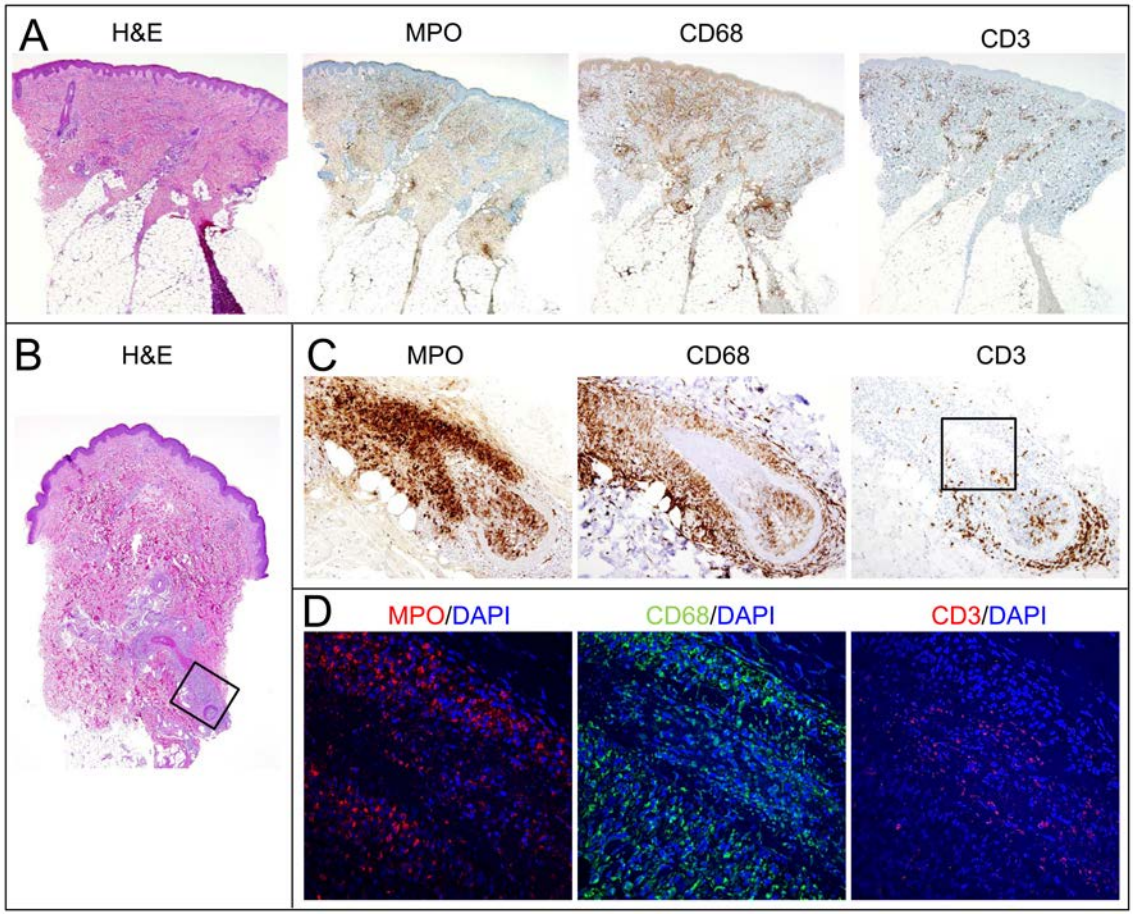

Figure S1. Skin Manifestations in Patients with ADA2 Mutations

A) The first panel shows H&E staining in the skin biopsy from the left forearm of Patient 3 (40X magnification). The second to fourth panels show a predominantly interstitial dermal inflammatory infiltrate composed of MPO^+ neutrophils and $CD68^+$ macrophages and a perivascular lymphocytic inflammatory infiltrate composed of predominantly $CD3^+$ lymphocytes (T cells). (MPO, myeloperoxidase; 40X original magnification)

B) Hematoxylin and eosin (H&E) staining in the skin biopsy from Patient 4 (40X magnification). The square indicates the area showing the following immunostaining images (C-D).

C) Immunohistochemistry staining for MPO, CD68 and CD3 in Patient 4. Positive cells are stained brown and nuclei are shown as blue by counterstaining with hematoxylin. (200X magnification). The square indicates the area showing the following immunostaining images in panel D.

D) Immunofluoresence staining for MPO (myeloperoxidase; red), CD68 (green) and CD3 (red) in Patient 4 (400X magnification). Nuclei are stained blue with DAPI.

Figure S2

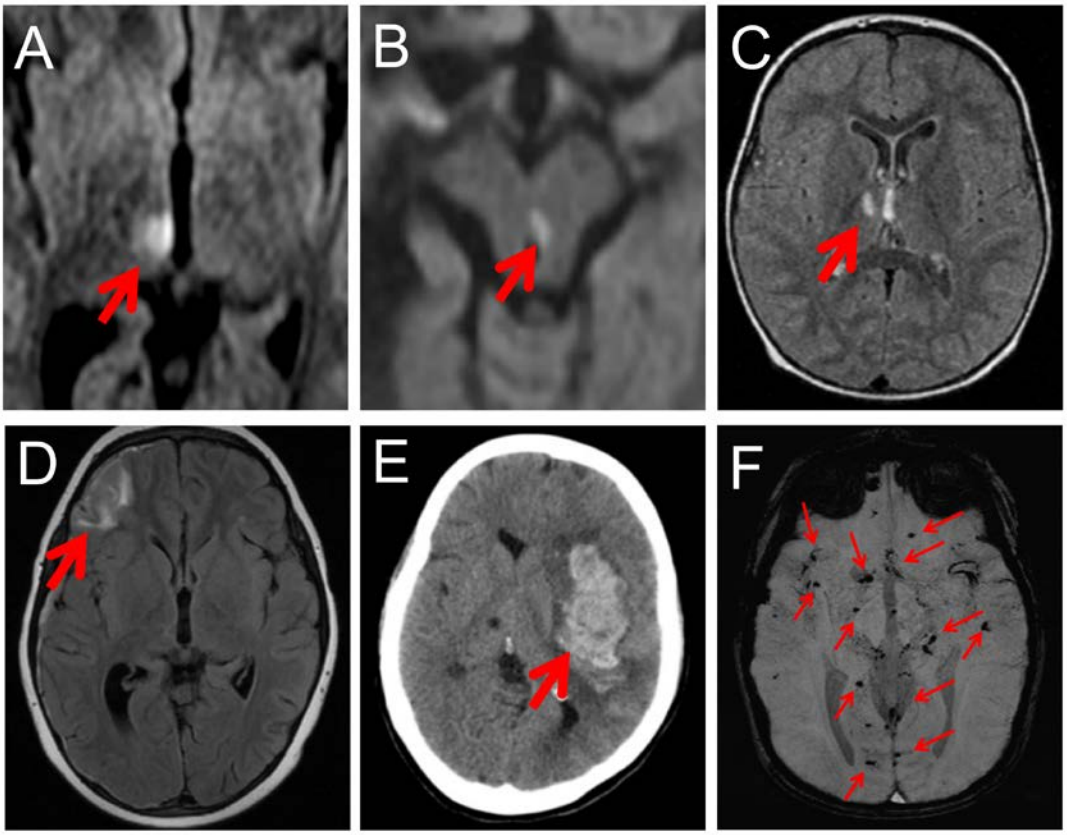

Figure S2: Brain Imaging

A-B) DWI axial MRI images were collected four months apart from each other illustrating the multifocal nature of small vessel acute brain ischemia in Patient 3 (corresponding ADC maps are not included). Figure 1E in the text depicts an area of acute ischemia in the left paramedian midbrain in Patient 3 at a time point two months after the MRI in panel A of this figure.

C) Area of abnormal T2 signal hyperintensity on FLAIR imaging consistent with a subacute small vessel ischemic event over the right internal capsule and thalamus in Patient 1.

D) Localized areas of T2 hyperintensity on FLAIR images, worse over the right anterior convexity, involving intracranial, subarachnoid, and subdural spaces due to hemorrhage in Patient 3.

E) Unenhanced CT scan of the brain demonstrating a large acute left intracranial hematoma with mass effect at age 22 in Patient 4.

F) Susceptibility weighted imaging demonstrates multiple small foci of decreased signal intensity along the folding of cortical sulci in Patient 5. These changes are most consistent with hemosiderin deposits from previous subarachnoid hemorrhage.

DWI, Diffusion Weighted Imaging; ADC, Apparent Diffusion Coefficient; FLAIR, Fluid Attenuation Inversion Recovery.

Figure S3

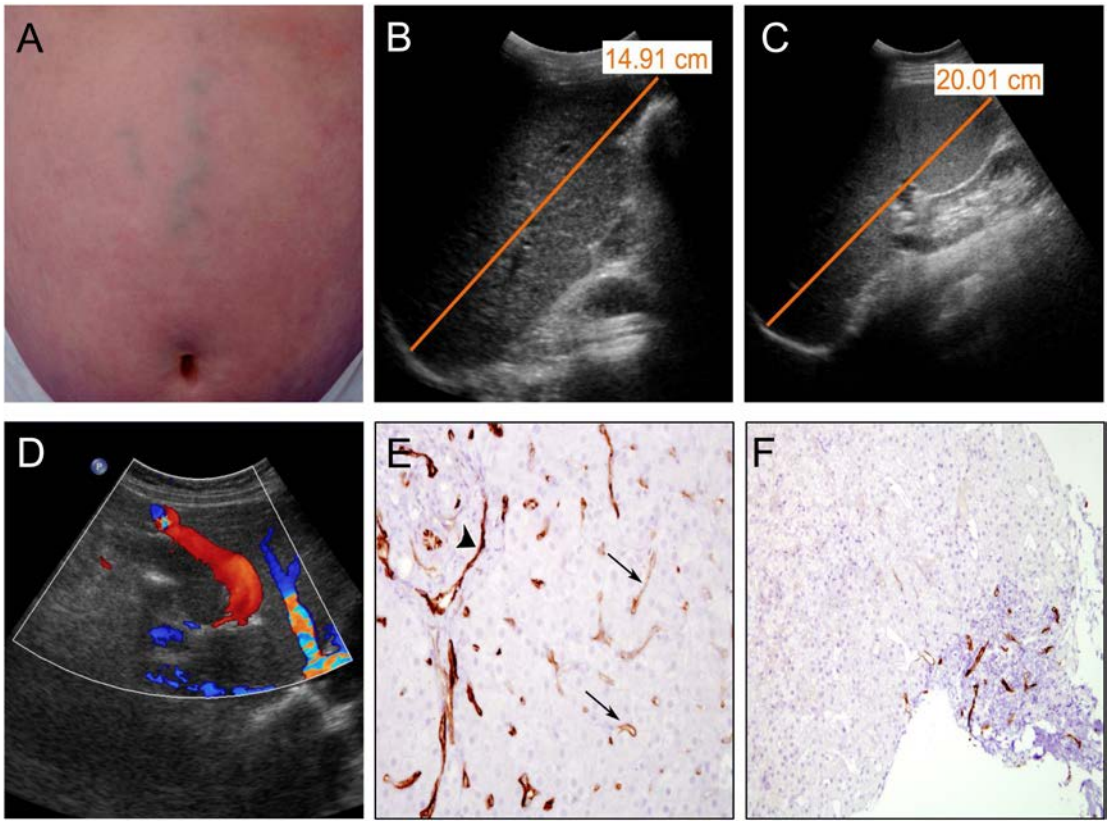

Figure S3. Hepatosplenomegaly and Liver Findings

A) Congested collateral vein near the umbilicus in Patient 2.

B-C) Sonographic images of the liver (B), and spleen (C) in patient 4 demonstrate splenomegaly and liver span at upper limits of normal. 15 cm is upper limit of normal liver and 14 cm is upper limit of normal spleen.

D) Transverse color-flow Doppler ultrasound image of the left liver demonstrating hepatofugal flow between left portal vein and patient's umbilical vein (large red vessel) in Patient 2.

E-F) Photomicrograph of hepatoportal sclerosis in liver biopsy tissue from Patient 2 showing aberrant staining of sinusoidal endothelium with anti-CD34 antibody

(arrows). Within the portal area, the portal vein is slit-like (arrowhead). Control sample is from a patient with unrelated liver pathology and shows only staining of portal vessel endothelium (F). (anti-CD34, 200X)

Figure S4

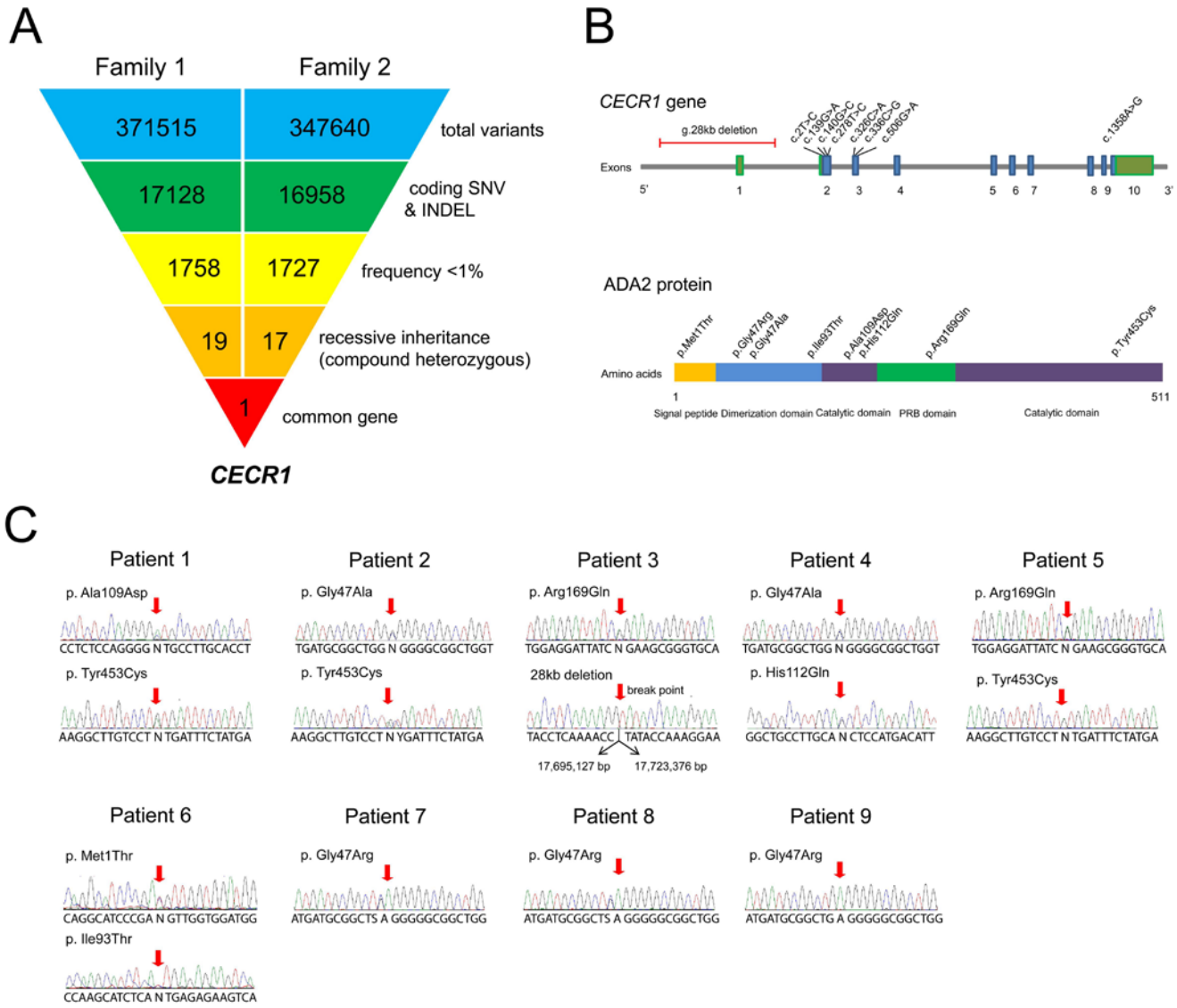
A
Family 1
Family 2
371515
347640
total variants
17128
16958
coding SNV & INDEL
1758
1727
frequency <1%
19
17
recessive inheritance (compound heterozygous)
1
common gene
CECR1
B
CECR1 gene
g.28kb deletion
c.-2T>C
c.139G>A
c.140G>C
c.276T>C
c.336C>A
c.336C>G
c.506G>A
c.1358A>G
Exons
5'
1
2
3
4
5
6
7
8
9
10
3'
ADA2 protein
p.Met1Thr
p.Gly47Arg
p.Gly47Ala
p.Ile93Thr
p.Ala109Asp
p.His112Gln
p.Arg169Gln
p.Tyr453Cys
Amino acids
1
511
Signal peptide
Dimerization domain
Catalytic domain
PRB domain
Catalytic domain
C
Patient 1
p. Ala109Asp
CCTCTCCAGGGG N TGCCTTGCACCT
p. Tyr453Cys
AAGGCTTGTCCT N TGATTTCTATGA
Patient 2
p. Gly47Ala
TGATGCGGCTGG N GGGGCGGCTGGT
p. Tyr453Cys
AAGGCTTGTCCT N YGATTTCTATGA
Patient 3
p. Arg169Gln
TGGAGGATTATC N GAAGCGGGTGCA
28kb deletion
break point
TACCTCAAAACC TATACCAAAGGAA
17,695,127 bp
17,723,376 bp
Patient 4
p. Gly47Ala
TGATGCGGCTGG N GGGGCGGCTGGT
p. His112Gln
GGCTGCCTTGCA N CTCCATGACATT
Patient 5
p. Arg169Gln
TGGAGGATTATC N GAAGCGGGTGCA
p. Tyr453Cys
AAGGCTTGTCCT N TGATTTCTATGA
Patient 6
p. Met1Thr
CAGGCATCCCGA N GTTGGTGGATGG
p. Ile93Thr
CCAAGCATCTCA N TGAGAGAAGTCA
Patient 7
p. Gly47Arg
ATGATGCGGCTS A GGGGGCGGCTGG
Patient 8
p. Gly47Arg
ATGATGCGGCTS A GGGGGCGGCTGG
Patient 9
p. Gly47Arg
ATGATGCGGCTG A GGGGGCGGCTGG

Figure S4. Whole Exome Sequencing Approach and *CECR1* Mutations

A) Schematic representation of the exome data-filtering approach assuming recessive inheritance in Families 1 and 2, leading to the identification of *CECR1* as the causative gene in these families. SNV: single nucleotide variants including missense variants, splice site variants, and stop codon variants; INDEL, frame shift and non-frame shift insertions and deletions.

B) Positions of the identified mutations within the *CECR1* gene (upper) and the corresponding locations of missense changes within the protein domains of ADA2 (lower).

C) Electropherograms for the *CECR1* mutations identified in 9 patients with ADA2 deficiency. The deletion was identified on a high-density SNP bead-chip array (HumanOmniExpress, Illumina), and the deletion breakpoint in Patient 3 was sequenced with primers designed from each end of the boundaries identified through the analysis of SNPs.

Figure S5

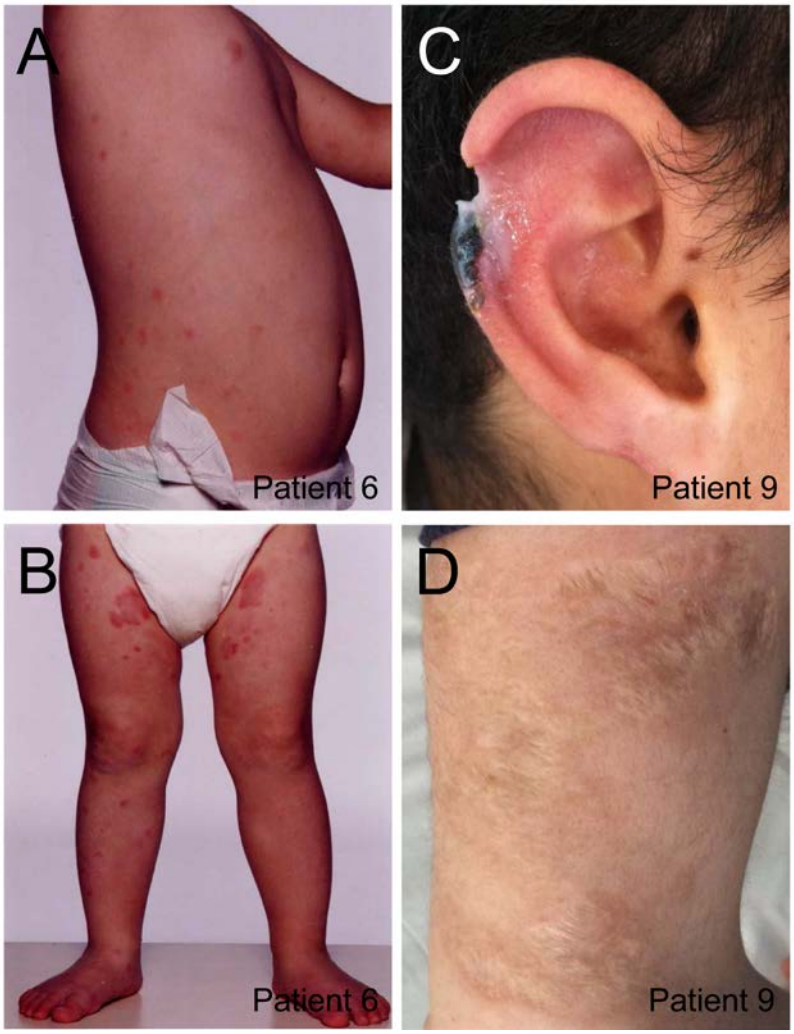

Figure S5. Dermatologic Manifestations in Patient 6 and Patient 9

A-B) As an infant patient 6 presented with transient, recurrent skin rash: erythematous dermal nodules and plaques in lower trunk and thighs.

C) Necrotizing lesion in the ear lobe leading to tissue loss in Patient 9.

D) Scarred tissue of a healing vasculitic lesion on the arm of Patient 9.

Figure S6

A

SNP	Position	Patient 1		Patient 2		Patient 3		Patient 4		Patient 5	
		A109D	Y453C	G47A	Y453C	R169Q	Deletion	G47A	H112Q	R169Q	Y453C
rs7288562	17661764	A	A	G	A	A	A	G	A	A	A
rs200383408	17661791	G	G	A	G	G	G	A	G	G	G
rs7289697	17661922	G	G	C	G	G	G	C	G	G	G
rs11704850	17661935	T	T	A	T	T	T	A	T	T	T
rs7290147	17662163	G	C	C	C	G	G	C	G	G	C
rs41282461	17662679	G	G	A	G	G	G	A	G	G	G
rs58754958	17662699	T	T	C	T	T	T	C	T	T	T
rs7289170	17662793	T	T	C	T	T	T	C	T	T	T
Y453C	17662794	A	**G**	A	**G**	A	A	A	A	A	**G**
rs3764846	17662917	C	C	G	C	C	C	G	C	C	C
rs7284498	17669199	C	T	C	T	C	C	C	C	C	T
rs2231495	17669306	A	G	G	G	A	A	G	A	A	G
rs9619005	17669406	C	G	G	G	C	G	G	C	C	G
rs9617966	17669469	A	G	A	G	G	A	A	A	G	G
rs141611354	17669497	A	A	A	A	A	A	A	A	A	A
rs11704246	17669641	A	A	A	A	A	A	A	A	A	A
rs13053147	17669686	T	C	C	C	C	C	C	T	C	C
rs2286347	17671052	G	G	G	G	G	G	G	G	G	G
rs5747022	17684355	C	C	C	T	T	C	C	C	T	T
R169Q	17687997	G	G	G	G	**A**	G	G	G	**A**	G
H112Q	17688167	C	C	C	C	C	C	C	**G**	C	C
A109D	17688177	**A**	C	C	C	C	C	C	C	C	C
rs362129	17690409	T	T	C	C	C	T	C	T	C	C
G47A	17690428	G	G	**C**	G	G	G	**C**	G	G	G
rs7289141	17690430	G	G	G	G	G	G	G	G	G	G
rs713684	17702505	C	C	C	T	T	**X**	C	C	T	T
rs2079621	17702580	A	G	G	A	A	**X**	G	A	A	A
rs737968	17702662	G	G	G	G	G	**X**	G	G	G	G
rs737967	17702778	G	A	A	A	A	**X**	A	G	A	A
rs3884692	17702858	G	A	A	G	G	**X**	A	G	G	G
rs737966	17702876	C	C	C	A	A	**X**	C	C	A	A

B

SNP	Position	Patient 7		Patient 8		Patient 9	
		G47R	G47R	G47R	G47R	G47R	G47R
rs11704850	17661935	T	A	T	A	T	T
rs7290147	17662163	G	C	G	C	G	G
rs41282461	17662679	G	A	G	A	G	G
rs58754958	17662699	T	C	T	C	T	T
rs7289170	17662793	T	C	T	C	T	T
rs3764846	17662917	C	G	C	G	C	C
rs2231496	17669151	A	A	A	A	A	A
rs9619005	17669406	G	G	G	G	G	G
rs13053147	17669686	C	C	C	C	C	C
rs5747022	17684355	C	C	C	C	C	C
rs362129	17690409	T	C	T	C	T	T
G47R	17690429	**A**	**A**	**A**	**A**	**A**	**A**
rs7289141	17690430	G	C	G	C	G	G
rs2079621	17702580	A	A	A	A	A	A
rs737968	17702662	A	G	A	G	A	A

Figure S6. *CECR1* Mutation-Associated Haplotypes

A) *CECR1* haplotypes constructed from a set of 26 SNPs for patients 1-5.

Shared mutation-bearing haplotypes are indicated in different colors.

B) *CECR1* haplotypes constructed from a set of 15 SNPs for patients 7-9 of Turkish ancestry. The p.Gly47Arg mutation was found on two haplotypes. The haplotype shared among 3 patients from 2 families is indicated in green. Note a second shared haplotype in sibling patients 7 and 8.

Figure S7

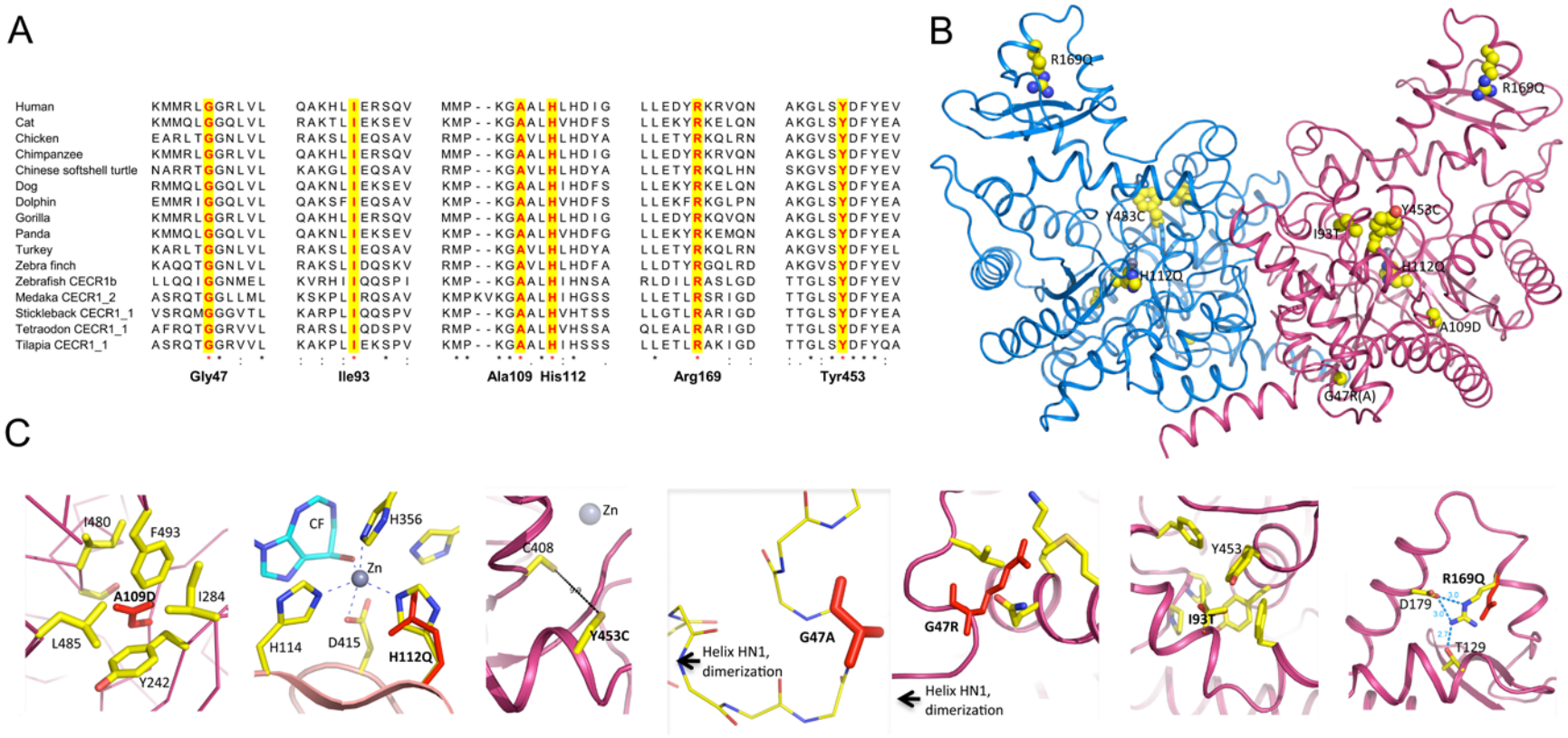

Figure S7. Evolutionary Conservation and *In silico* Modeling

A) Evolutionary conservation at the sites of Gly47, Ile93, Ala109, His112, Arg169, and Tyr453.

B) Location of the sites of mutations in the 3D structure of human ADA2[1]**.** The ADA2 dimer is shown as a ribbon diagram with the two subunits painted in magenta and marine. The residues mutated in patients are shown as spherical space-filling models. Amino acid numbering is based on the unprocessed sequence (+26 AA). The mutations occurred in critical positions in the catalytic domain (Ala109, His112, and Tyr453), dimerization domain (Gly47, Ile93) and the putative receptor-binding domain (Arg169)[1]. Carbon, oxygen, and nitrogen atoms are colored in yellow, red, and blue, respectively.

C) *In silico* modeling of ADA2 mutations based on the crystal structure of human ADA2**.** The amino acid side chains are shown as sticks. Native residues are colored by atom type as in (B) and mutations are shown in red. The three panels on the left depict mutations likely to affect the enzymatic activity or stability of the protein (p.Ala109Asp, p.His112Gln, p.Tyr453Cys). First panel, the best fit for the Ala109→Asp substitution. Note the highly hydrophobic surrounding of the negatively charged mutation (residues Tyr242, Ile284 and 480, Leu485, and Phe493), suggesting a low stability for such a structure. Second panel, the His112→Gln mutation distorts coordination of the catalytic Zn ion by deleting one coordination bond. The coformycin (CF) molecule, mimicking the substrate[1], and the Zn ion are shown as sticks and sphere, respectively. Third panel, Tyr453→Cys may cause distortion of the catalytic site structure by the formation of a Cys408-Cys453 disulfide bond. Note the close proximity of Cys408 and Cys453, as well as Cys408 and the catalytic Zn ion. The fourth, fifth, and sixth panels depict mutations likely to affect dimerization (p.Gly47Ala, p.Gly47Arg,

p.Ile93Thr). Fourth and fifth panels, Gly47→Ala and Gly47→Arg distorting the highly conserved Gly-Gly turn that is critical for the correct positioning of dimerization helix HN1[1] are shown in the fourth and fifth panels, respectively. Modeling of Ala in the position 47 results in high-energy conformation of the residue (ϕ and ψ angels 87.31 and -2.15, respectively). Modeling of Arg in the position 47, in addition, results in multiple clashes between the introduced bulky side chain and several residues (shown). In order to resolve these structural problems, the conserved GlyGly turn must be altered. Sixth panel, Ile93→Thr destabilizes the structure of the dimerization domain by deleting an important hydrophobic contact between α-helices. Seventh panel, Arg169→Gln destabilizes the structure of the putative receptor-binding domain, by deleting ionic and hydrogen bonds (indicated by dashed lines).

Figure S8

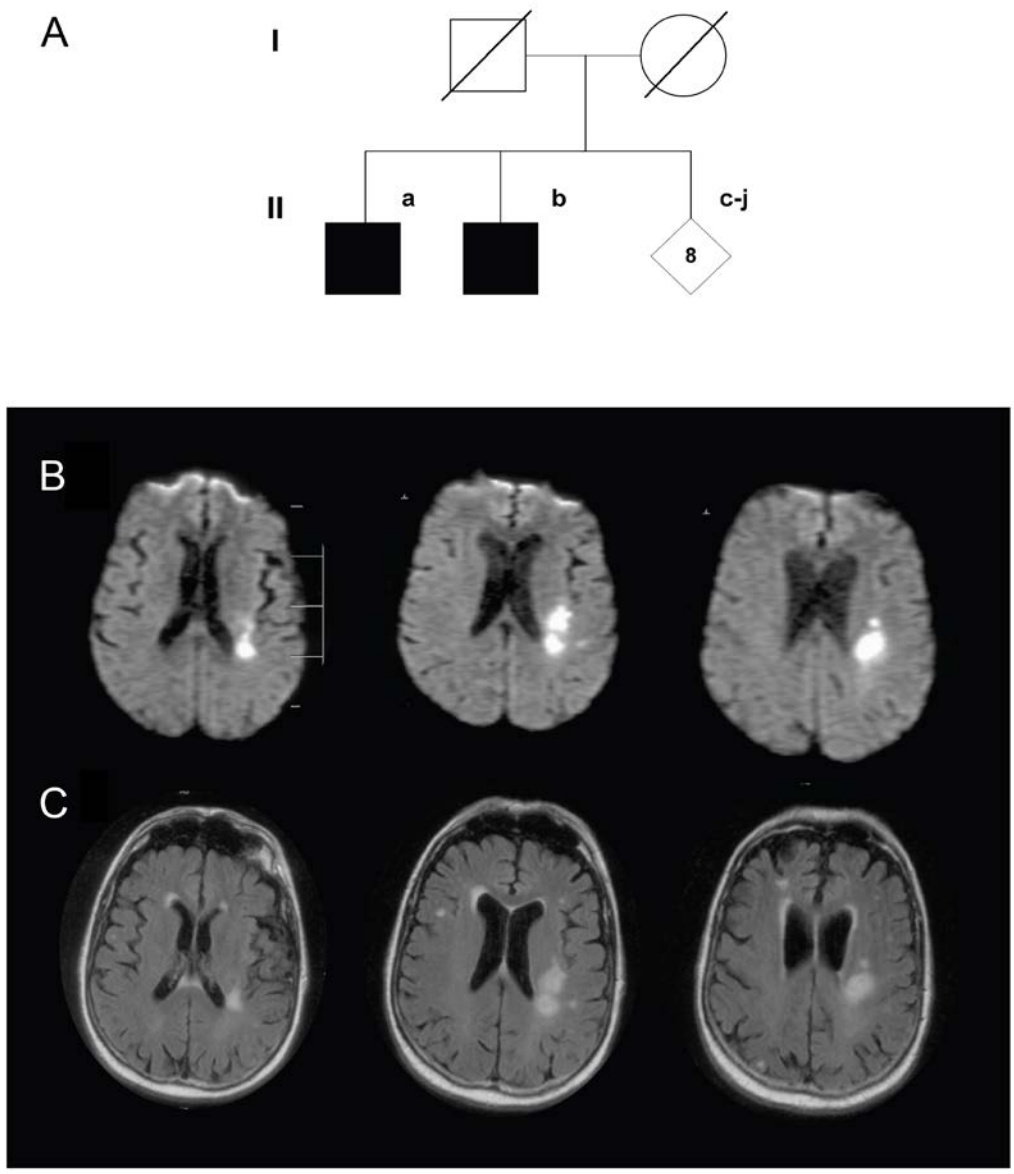

Figure S8. Small Vessel Ischemic Strokes in Adults Heterozygous for the p.Tyr453Cys Mutation

A) Pedigree diagram showing two brothers enrolled in the Siblings with Ischemic Stroke Study (SWISS) who both had small vessel ischemic strokes and carry the p.Tyr453Cys mutation.

B, C) Case II-b was a 79-year-old Portuguese man without prior neurological history who presented with right-sided facial droop that progressed to right hemiparesis. He had a history of hypertension, hyperlipidemia, and colon cancer status post resection and chemotherapy. He was taking metoprolol, clonidine, atorvastatin, triamterene, and hydrochlorothiazide. He did not smoke cigarettes and consumed 2 alcoholic beverages/day. Blood pressure was 184/78 mmHg; pulse, 74 beats/min; and temperature, 36.3 deg. C. He had right lower facial droop. Right upper and lower limb strength was 3 to 4/5. He had numbness to light touch and cold temperature sensation on the right side of the face and the right upper and lower limbs along with loss of vibration on the right. Brain diffusion-weighted (B) and FLAIR images (C) showed multifocal acute infarcts in the left middle cerebral arterial territory. Carotid ultrasound showed no significant stenosis. Echocardiography showed no embolic source. Ambulatory electrocardiography showed no atrial fibrillation. Despite taking aspirin and clopidogrel, the patient developed transient worsening of symptoms during hospitalization, which led to discontinuation of the antiplatelet therapy and initiation of warfarin. Seven days later, with an INR of 2.25, he had a 25 minute relapse of symptoms.

Figure S9

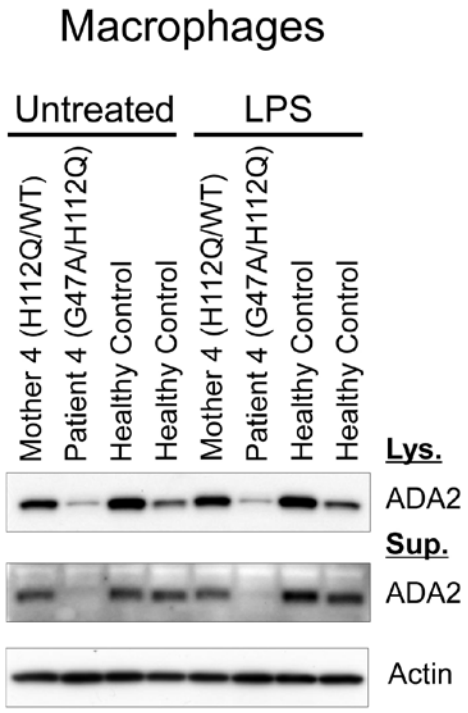

Figure S9. ADA2 Expression in Cultured Patient Macrophages

Differentiated macrophages from Patient 4, her heterozygous carrier mother, and two healthy controls were stimulated *ex vivo* with lipopolysaccharide (LPS) and cell lysates and supernatants were immunoblotted with polyclonal antibody for ADA2. Similar results were obtained in cultured macrophages from all five NIH patients.

Figure S10

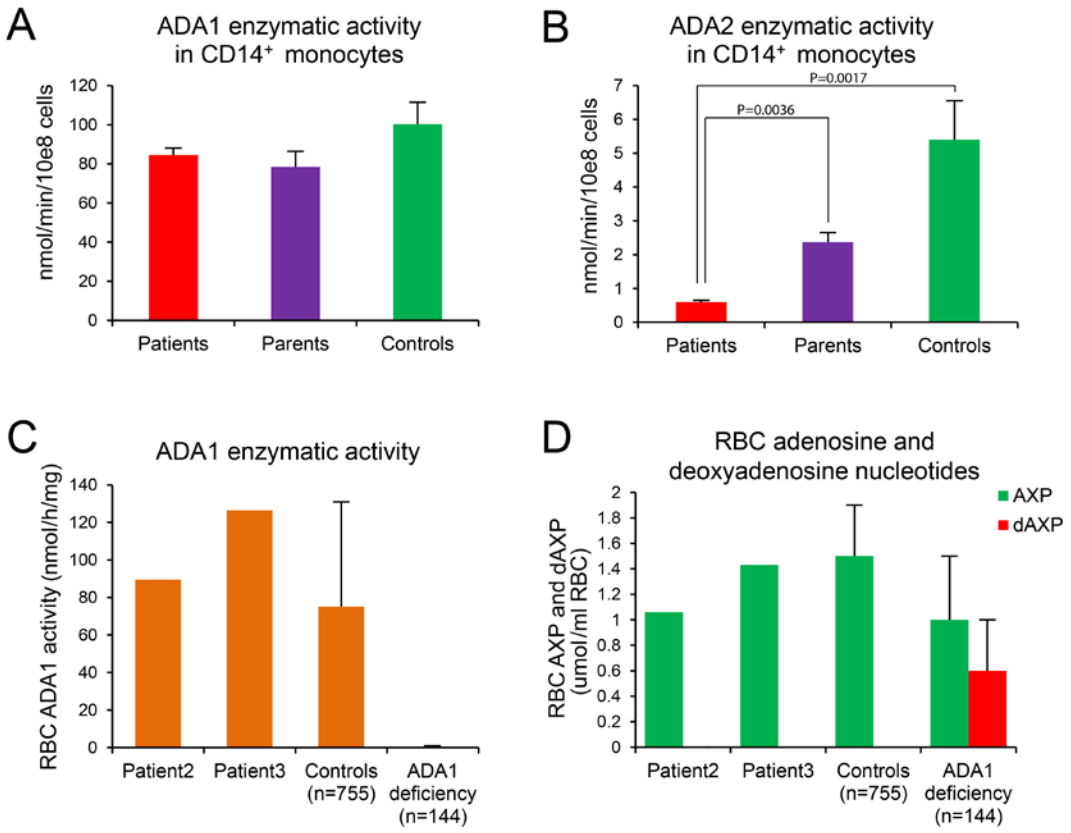

Figure S10. ADA1 and ADA2 Enzymatic Activity

A-B) ADA1 and ADA2 enzymatic activity was assayed in lysates from $CD14^+$ purified monocytes in Families 3 and 5. Normal ranges were established from the blood samples of 12 healthy donors.

C) ADA1 deaminase activity was assayed in hemolysates from Patients 2 and 3, 755 healthy controls, and in patients with ADA1 deficiency.

D) Total adenosine (green bars) and deoxyadenosine nucleotides (red bars) measured as an absolute quantity, in erythrocyte lysates from Patients 2 and 3, healthy controls, and 144 patients with ADA1 deficiency.

Figure S11

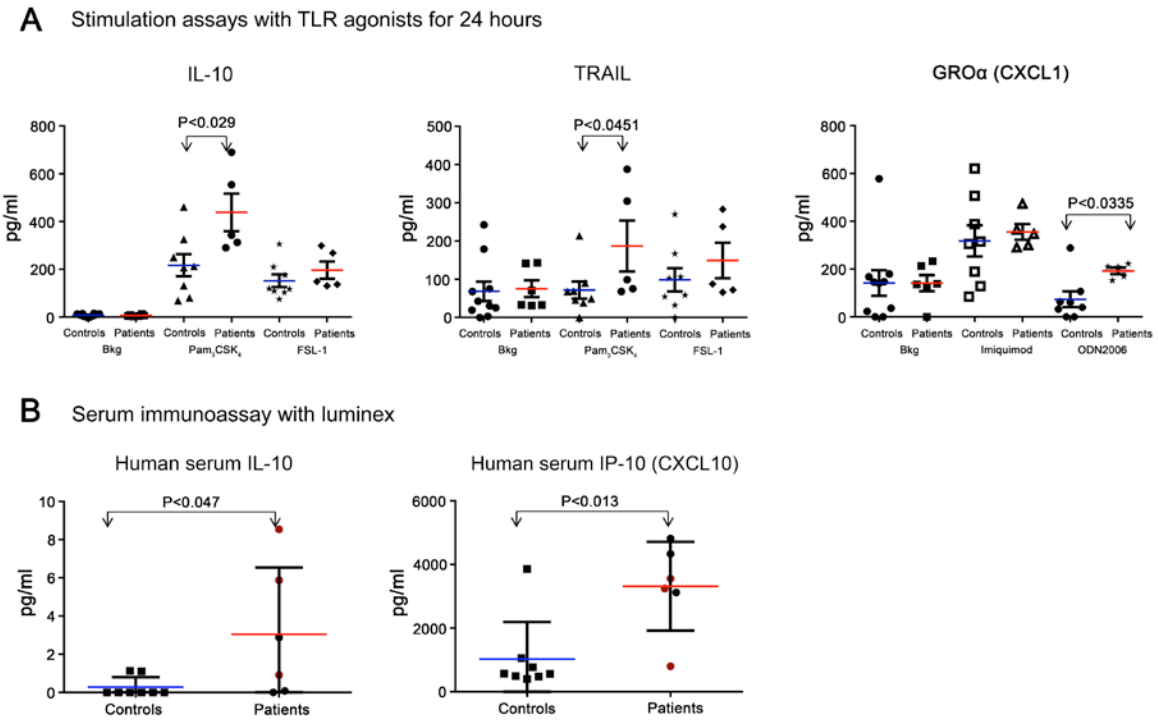

Figure S11. Cytokine Profiles Comparing ADA2-Deficient Patients with Healthy Controls

A) Supernatants of cells from whole blood stimulated with various TLR ligands for 24 h, from each of the 5 ADA2-deficient NIH patients, compared with 8 – 10 healthy controls. A total of 48 cytokines or growth factors were assayed, and are listed in the Supplemental Methods. The data shown here are the only comparisons that achieved nominal statistical significance by the Mann-Whitney test, which would not withstand correction for multiple comparisons.

B) Bead-based immunoassay for 27 cytokines or growth factors in the serum of 5 ADA2-deficient patients, compared with 8 healthy controls. The data here are

the only comparisons that achieved nominal statistical significance by the Mann-Whitney test, which would not withstand correction for multiple comparisons.

Figure S12

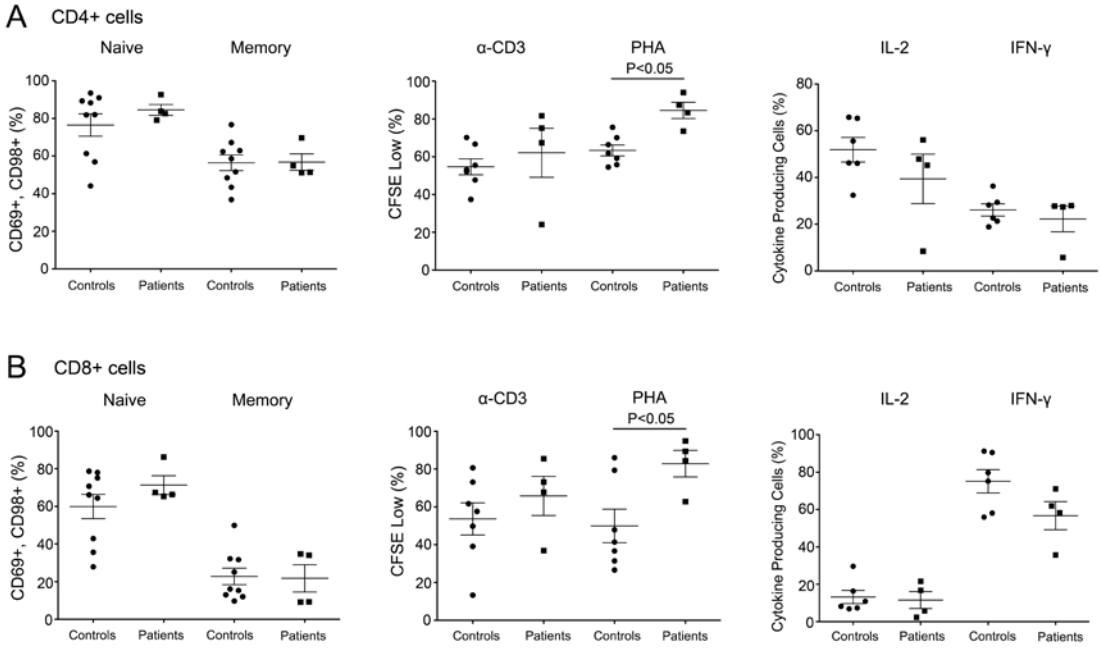

Figure S12. T Cell Activation, Proliferation, and Cytokine Secretion in ADA2 Deficiency

(Left) Short-term activation of naïve and memory cells as assessed by surface upregulation of CD69 and CD98 after overnight stimulation of PBMCs with anti-CD3, and then gating for $CD4^+$ (upper panel) or $CD8^+$ (lower panel) T cells.

(Middle) $CD4^+$(upper panel) and $CD8^+$ (lower panel) proliferative responses to anti-CD3 and phytohemagglutinin (PHA) stimulation after five days, measured by percentage of cells exhibiting CFSE dilution.

(Right) *Ex-vivo* cytokine production of IFN-γ and IL-2 after overnight stimulation with phorbol 12-myristate 13-acetate (PMA)/ionomycin. Percentages shown are of total memory populations ($CD45RO^+CD27^+$, $CD45RO^+CD27^-$ and $CD45RO^-$ CD27- combined), for $CD4^+$ (upper panel) and $CD8^+$ (lower panel) T cells.

Figure S13

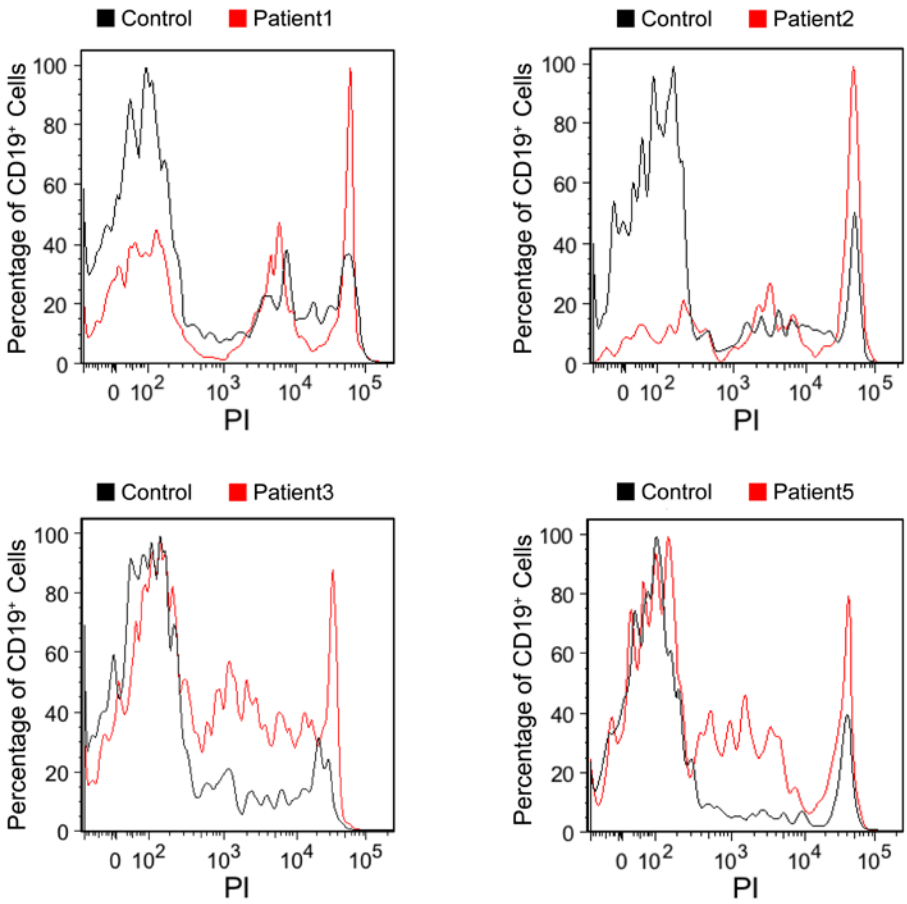

Figure S13. B cell Apoptosis Assay

Propidium iodide (PI) staining of $CD19^+$ B cells from 4 NIH patients and 4 healthy controls cultured for 48 hours, demonstrating higher rates of spontaneous cell death in patients' B cells. Thus, the first peak in each histogram identifies live cells that are PI negative. Patients' B cells (red line) show markedly increased spontaneous cell death compared to control cells (black line) and that is reflected by a larger proportion of patients' B cells in the PI positive peaks (dead cells) and a smaller proportion in the PI negative peaks (live cells).

Figure S14

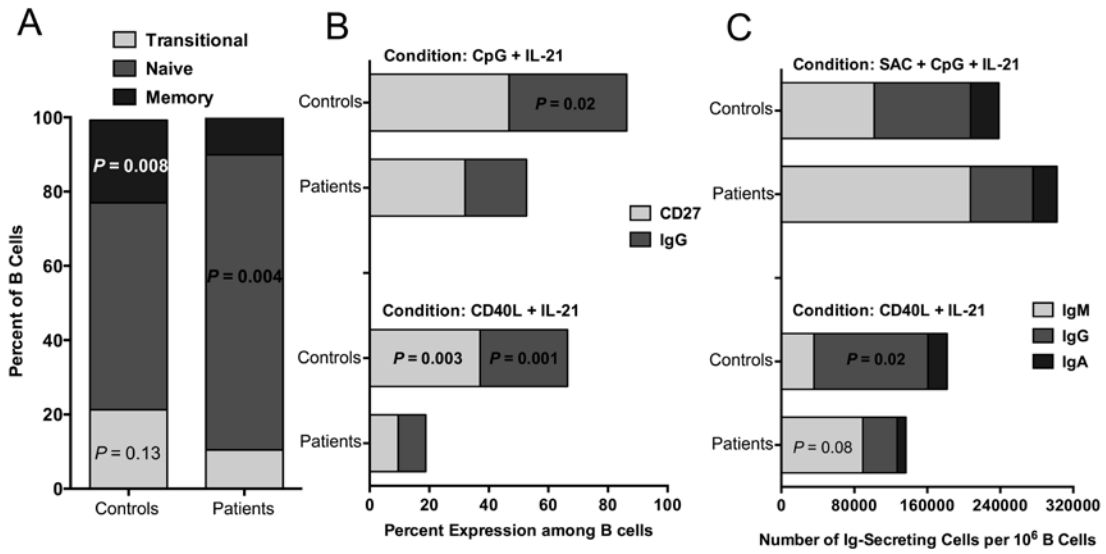

Figure S14. B Cell Subsets and Function in ADA2 Deficiency

A) Phenotypic analysis of B cells in the peripheral blood of 4 NIH ADA2-deficient patients and 5 age-matched healthy controls. *P*-values were determined for each subset and are shown in the group with the higher frequency.

B) Proliferation of PBMC B cells in response to the two conditions specified. Shown are the percentages of B cells at day 5 that express CD27 or IgG. *P*-values were determined for each marker and are shown in the group with the higher percent expression.

C) ELISPOT-based evaluation of the capacity of PBMC B cells to secrete immunoglobulins in culture following stimulation with the conditions shown. *P*-values were determined for each Ig and are shown in the group with the higher number.

Figure S15

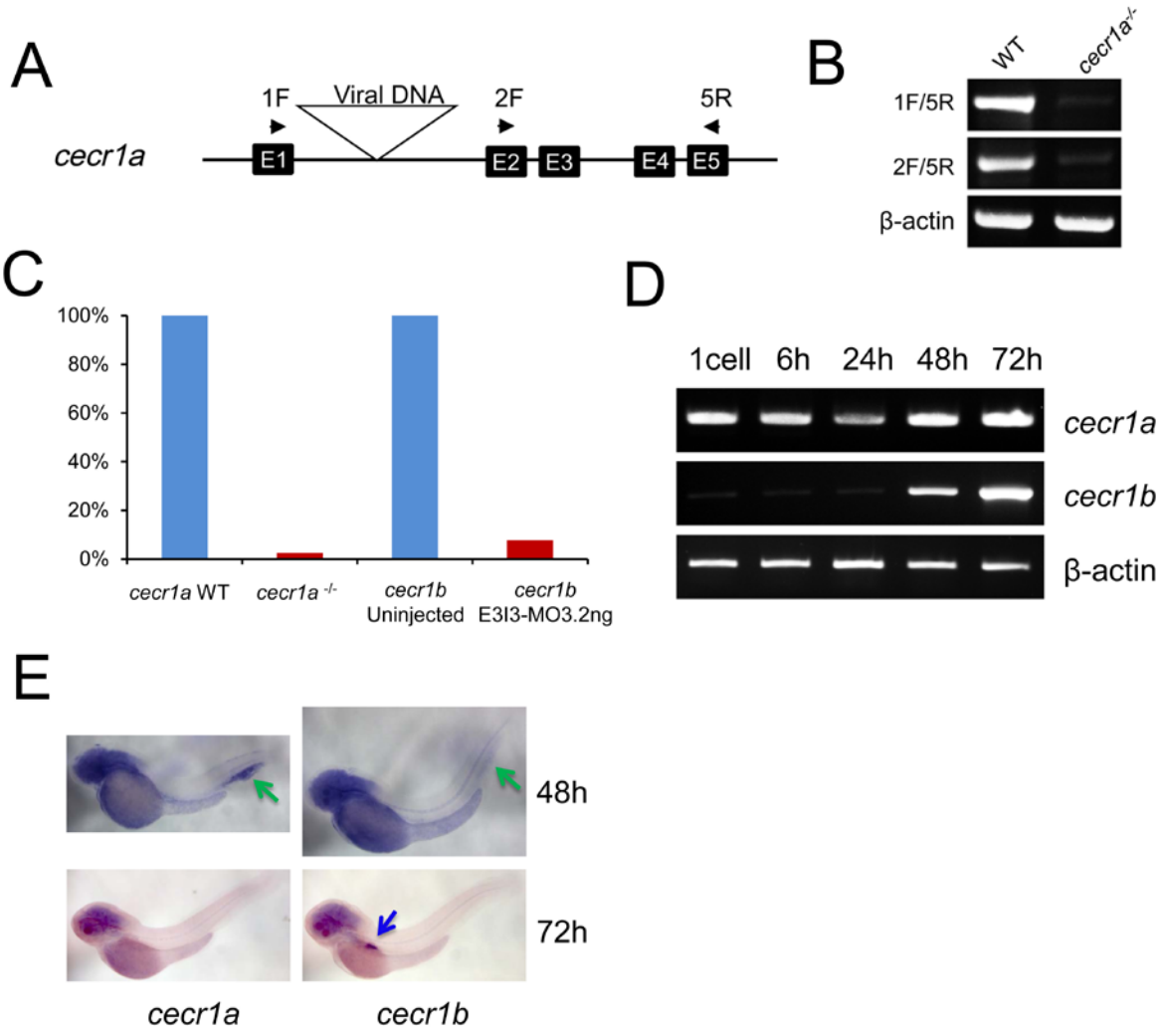

Figure S15. *cecr1a and cecr1b* Gene Expression in the Zebrafish

A) Mutant zebrafish line (la023164) with a retroviral integration in intron 1 of *cecr1a.*[13]

B) Reverse-transcriptase polymerase chain reaction (RT-PCR) analysis of the integration mutant line demonstrating a marked reduction in *cecr1a* expression in both the full-length (1F/5R) and potentially truncated (2F/5R) transcripts.

C) Quantitative RT-PCR to measure the levels of knockdown in *cecr1a* mutants and *cecr1b* morphants (E3I3-MO morpholino-injected embryos). *cecr1a* mutants showed <3% of wildtype expression, the *cecr1b* morphants showed ≈8% wildtype expression at 72 hours post fertilization (hpf).

D) RT-PCR for five embryo development stages (1 cell, 6 hpf, 24 hpf, 48 hpf, and 72 hpf) demonstrates different expression patterns of *cecr1a* and *cecr1b* during embryonic development.

E) In situ hybridization demonstrates *cecr1a* and *cecr1b* specific expression. Left panels indicate *cecr1a* expression mainly in the head at 48 hpf and 72 hpf, and vessel plexus at 48 hpf (green arrow). Right panels indicate *cecr1b* expression mainly in the head at 48 hpf and 72 hpf, in intestinal bud (blue arrow) at 72 hpf, and weak expression in vessel plexus at 48 hpf (green arrow). *cecr1a* and *cecr1b* are both expressed at low level in notochord at 48 hpf.

Figure S16

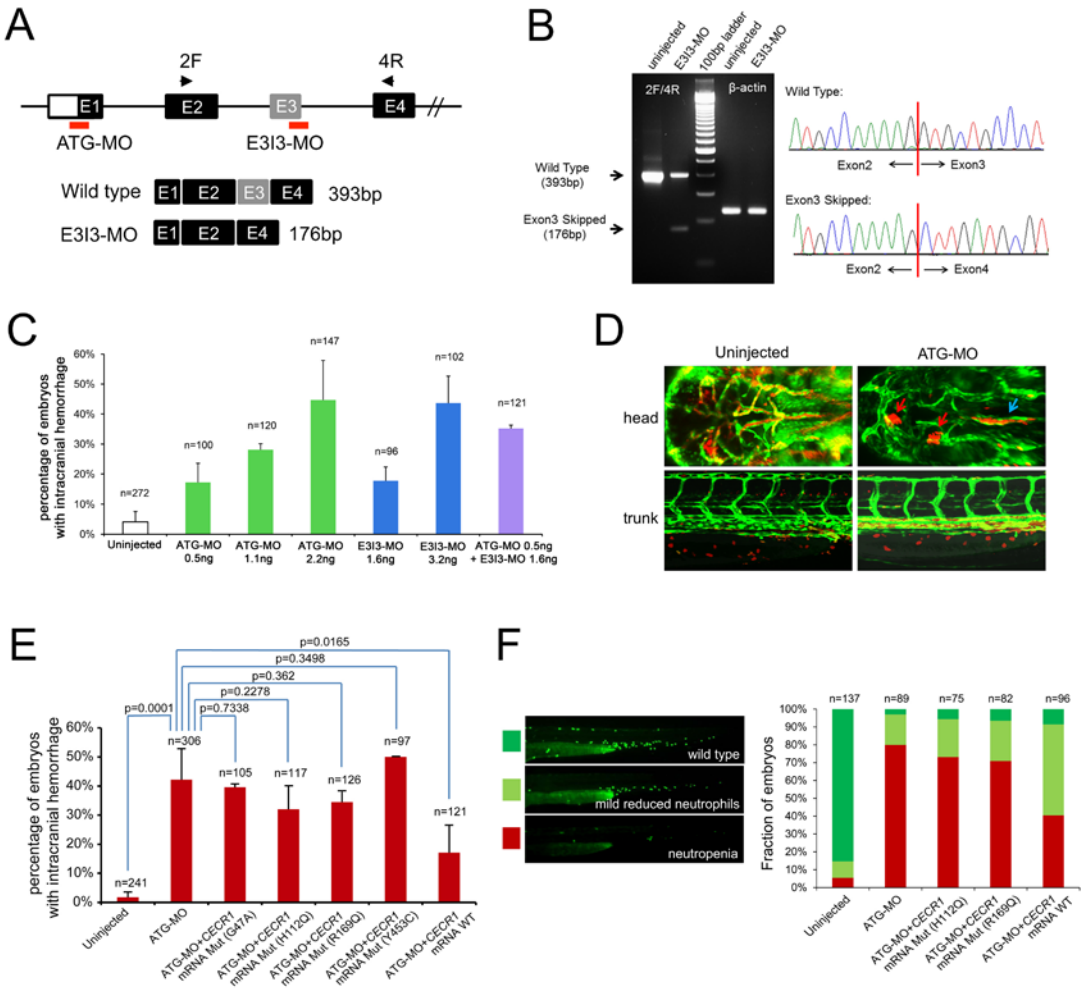

Figure S16. Functional Analysis of the *cecr1b* Gene in the Zebrafish

A) The zebrafish *cecr1b* gene was targeted by two specific morpholino antisense strategies to prevent either the translation of the zebrafish gene (ATG-MO) or proper splicing of exon 3 (E3I3-MO). Primers 2F and 4R interrogate the presence of wild type (non-mutant) transcripts or those in which exon 3 has been skipped. Below the diagram is a schematic depiction of the exon 3-skipped transcript in the E3I3-MO–injected embryos (176 bp) as compared with uninjected embryos (393 bp).

B) Left: RT-PCR of *cecr1b* transcript from uninjected and E3I3-MO morpholino-injected embryos 3 days after fertilization, demonstrating skipping of exon 3. Right: Sanger sequencing of both the wild type band and the exon 3-skipped band validating the wild type sequence and the exon 3-skipped sequence. Quantitative measurements of *cecr1b* expression levels measured by qRT-PCR are shown in Figure S15C.

C) Percentage of embryos with intracranial bleeding observed at varying doses of injected ATG-MO or E3I3-MO. Three experiments were performed to derive the percentages, with the total number of embryos studied in the three experiments listed as the *n* above each bar of the graph.

D) Confocal images of the trunk and head vessels at 48 hpf for uninjected and ATG-MO morpholino-injected embryos demonstrate grossly normal development in the growth of intersomitic and cranial vessels. Red arrow in upper right panel: intracranial hemorrhage, with a collection of DsRed erythrocytes that, on live-mount imaging, is outside of the vasculature. Blue arrow in upper right panel: a zone of vascular constriction and, on live-mount imaging, impaired blood flow, indicating intracranial ischemia.

E) Intracranial hemorrhages in zebrafish injected with ATG-MO (2.2 ng/embryo) and coinjected either with wild type or mutant human *CECR1* mRNA (100 pg/embryo). Wild type *CECR1* rescued ATG-MO-induced intracranial hemorrhages more effectively than any of the mutant *CECR1* mRNAs. These data were derived from two independent experiments.

F) Neutrophils in *mpx*:EGFP zebrafish injected with ATG-MO (2.2 ng/embryo) and coinjected either with wild type or mutant human *CECR1* mRNA (100 pg/embryo). Wild type *CECR1* rescued ATG-MO-induced neutropenia, whereas R169Q and H112Q *CECR1* mutants did not. Three phenotypes were scored: neutropenia, a slight reduction in neutrophils, and normal presence of neutrophils. These data were derived from two independent experiments.

Figure S17

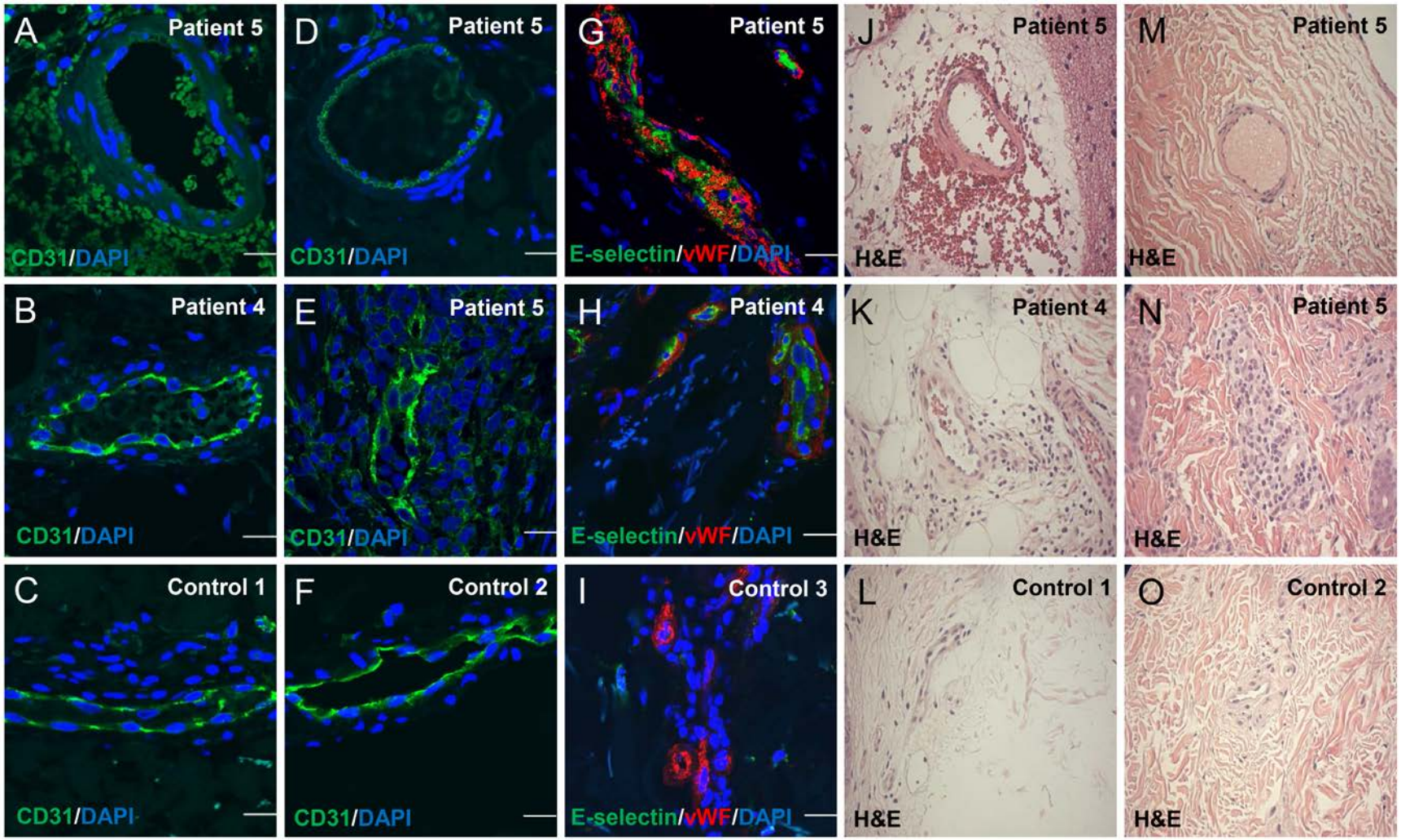
A
Patient 5
CD31/DAPI
D
Patient 5
CD31/DAPI
G
Patient 5
E-selectin/vWF/DAPI
J
Patient 5
H&E
M
Patient 5
H&E
B
Patient 4
CD31/DAPI
E
Patient 5
CD31/DAPI
H
Patient 4
E-selectin/vWF/DAPI
K
Patient 4
H&E
N
Patient 5
H&E
C
Control 1
CD31/DAPI
F
Control 2
CD31/DAPI
I
Control 3
E-selectin/vWF/DAPI
L
Control 1
H&E
O
Control 2
H&E

Figure S17. Immunohistochemistry of Brain and Skin Biopsies

A-F) Immunostaining of $CD31^+$ endothelial cells in brain (Panel A, D) and skin biopsy (Panel B, E) samples from Patient 4 and 5 and skin biopsy from a normal control donor (Panel C, F). Disruption of endothelial layer is present only in samples from ADA2 deficient patients. CD31 stained green. Nuclei are stained blue with DAPI. (Scale bar: 20 µm)

G-I) Endothelial cell activation marker E-selectin staining in brain biopsy from Patient 5 (Panel G), and skin biopsy sample from Patient 4 (Panel H) and a normal control donor (Panel I). E-selectin stained green. Endothelial cell marker von Willebrand factor (vWF) stained red. Nuclei are stained blue with DAPI. (Scale bar: 20 µm)

J-O) Panels J and M show H&E staining in brain biopsy samples from Patient 5. Panels K, L, N and O show H&E staining in skin biopsy samples from Patient 4 (Panel K), Patient 5 (Panel N) and two normal control donors (Panel L and O).

Figure S18

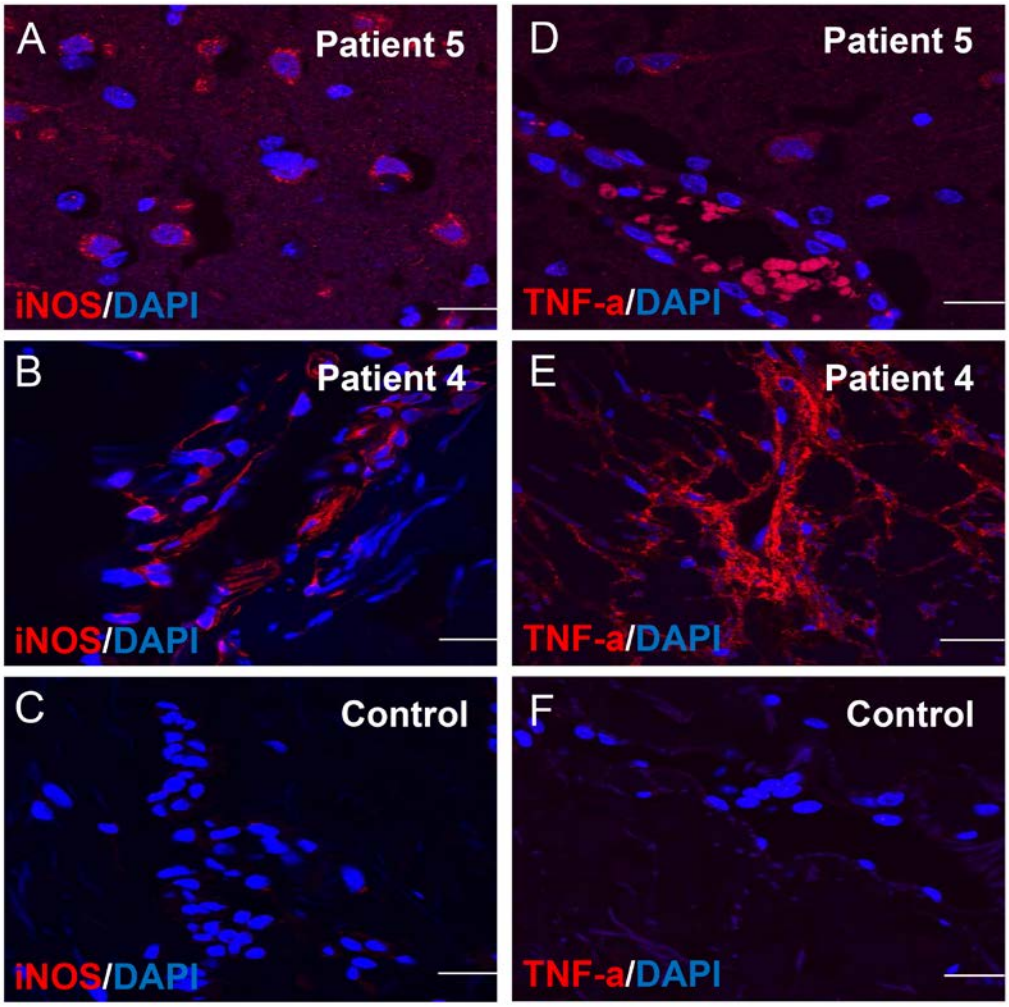

Figure S18. Immunostaining for Inflammatory Markers in Patients' Tissues

Inflammatory markers iNOS (A – C), and TNF-α (D – F) immunostaining in brain biopsy samples from Patient 5 (A, D) and skin biopsy samples from Patient 4 (B, E) and a control donor (C,F). iNOS and TNF-α are stained red. Panels A and D show positive-staining cells in the brain samples from Patient 5. Panels B and E show robust iNOS and TNF-α staining in Patient 4 skin samples. Nuclei are stained blue with DAPI. (Scale bar: 20 μm)

Figure S19

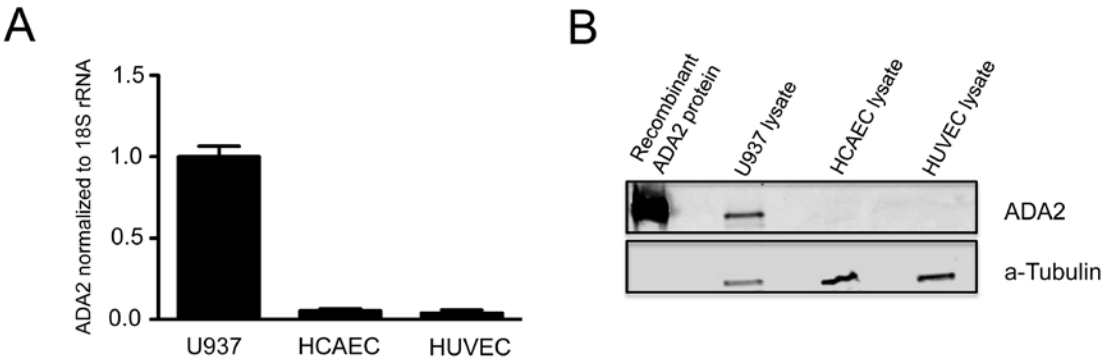

C

ID	Total (protein) ADA2 concentration, ng/ml	Active ADA2 concentration, ng/ml	SD
Controls	90 ± 24	108.965	3.665
HCAEC	≤ 1	≤ 1	/
HUVEC	≤ 1	≤ 1	/

Figure S19. *CECR1* Gene and Protein Expression and ADA2 Activity in Myeloid and Endothelial Cell Cultures

A) ADA2 mRNA expression levels in the myeloid cell line (U937), human coronary artery endothelial cells (HCAEC) and human umbilicord vein endothelial cells (HUVEC).

B) ADA2 protein expression levels in U937, HCAEC, and HUVEC.

C) ADA2 enzyme activity assay in HCAEC and HUVEC.

Figure S20

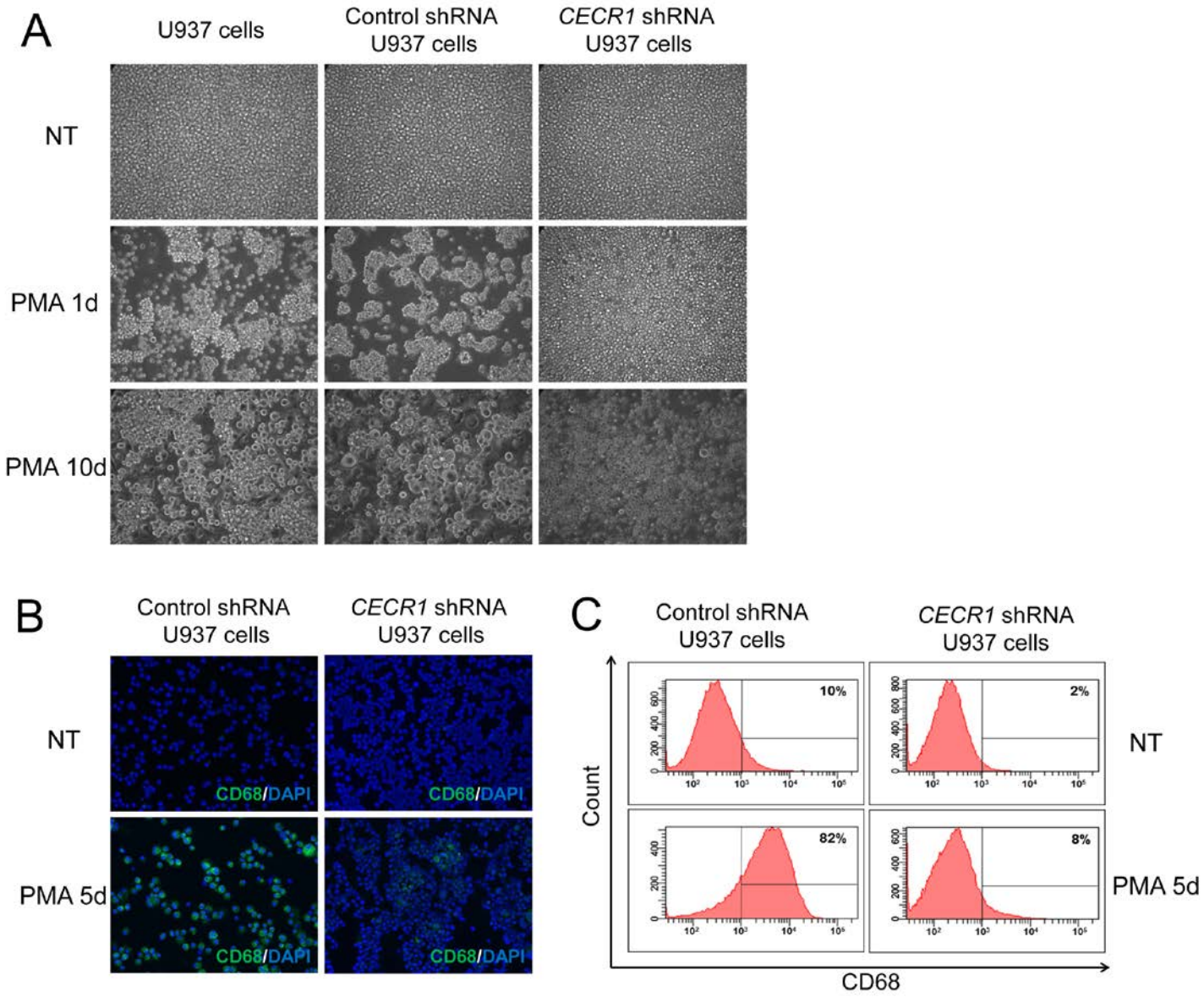
A
U937 cells
Control shRNA U937 cells
CECR1 shRNA U937 cells
NT
PMA 1d
PMA 10d
B
Control shRNA U937 cells
CECR1 shRNA U937 cells
NT
PMA 5d
CD68/DAPI
C
Control shRNA U937 cells
CECR1 shRNA U937 cells
10%
2%
82%
8%
NT
PMA 5d
Count
CD68

Figure S20. Differentiation of U937 Cells Into Macrophages by PMA and Immunostaining of Macrophage Marker CD68 in PMA-induced U937 Myeloid Cells

A) Human U937 myeloid cells, either non-transduced (left panels), transduced with control shRNA (middle panels), or with *CECR1* shRNA (right panels), were treated with PMA (20 ng/ml) for 1 day (middle panels) or 10 days (lower panels). NT, no treatment, shown in upper panels. *CECR1* shRNA-transduced U937 cells showed non-adherent cells with monocyte – like morphology, compared to non-transduced and control shRNA-transduced U937 cells that differentiated into adherent cells with typical macrophage morphology. (Image magnification: 200X)

B) Human U937 myeloid cells transduced with control shRNA (left panels), or with *CECR1* shRNA (right panels), were treated with (lower panels) or without (upper panels) PMA (20 ng/mL) for 5 days. Adherent and non-adherent cells were collected and cytospun for CD68 immunostaining (green). The majority of control shRNA U937 cells are CD68 positive after PMA treatment for 5 days (left lower panel). Only a few CD68 positive cells were observed in *CECR1* shRNA-treated U937 cells under PMA stimulation (right lower panel). Nuclei are stained blue with DAPI. NT, no treatment. (Image magnification: 200X)

C) ADA2 knockdown (*CECR1* shRNA) in U937 cells inhibits the expression of PMA-induced macrophage differentiation marker CD68 as shown by flow cytometry. NT, no treatment.

Figure S21

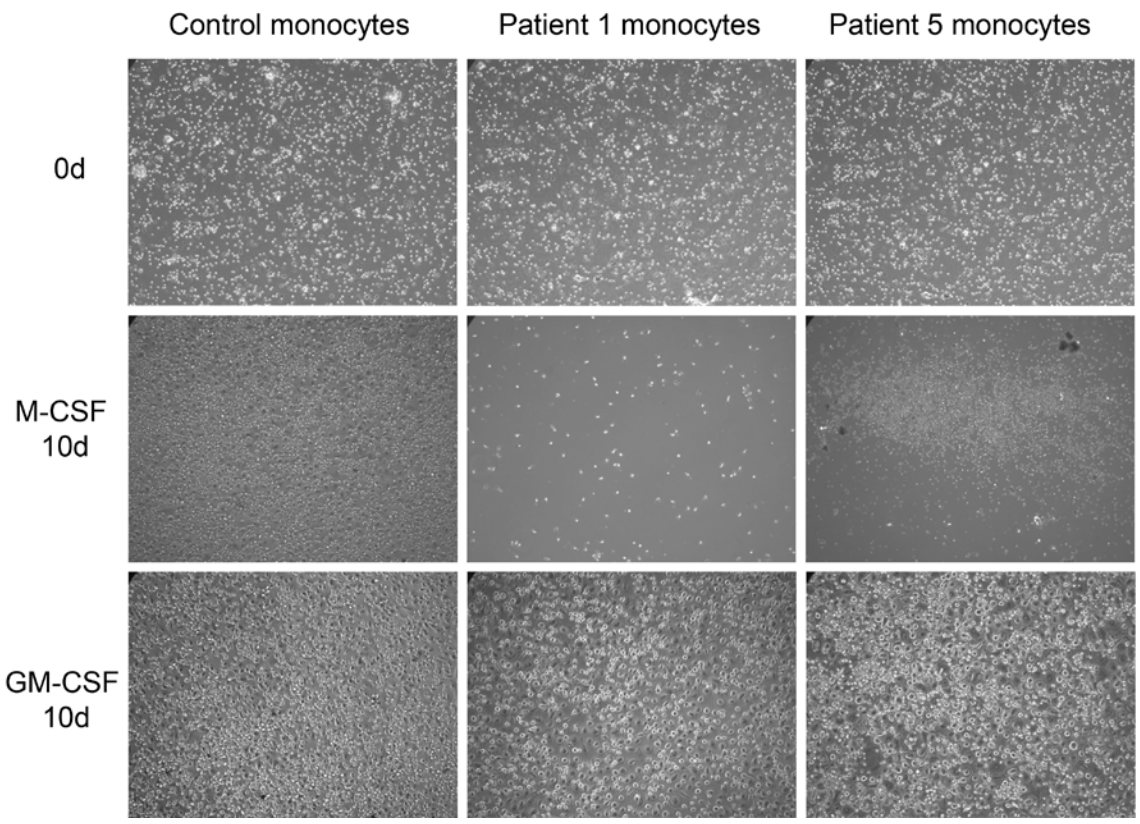

Figure S21. M-CSF and GM-CSF-Mediated Differentiation Assay in Isolated Monocytes

Monocytes were isolated by negative selection from patient and aged-matched control blood samples. Equal cell numbers were seeded and M2 macrophage differentiation was induced with 50 ng/ml of M-CSF while M1 macrophage differentiation was induced with 20 ng/ml GM-CSF for 10 days. Control monocytes attached and differentiated, exhibiting a macrophage-like morphology under both M-CSF and GM-CSF stimulation (left panel). Very few attached and differentiated M2-like cells were observed during the observation period in M-

CSF stimulated monocytes from Patient 1 (middle panel) and Patient 5 (right panel). However, M1-like GM-CSF-induced differentiation of monocytes from both patients was similar to control cells. The four panels in the lower left are also shown as Figure 4 G – J; they are repeated here for the sake of comparison. (Image magnification: 100X)

Figure S22

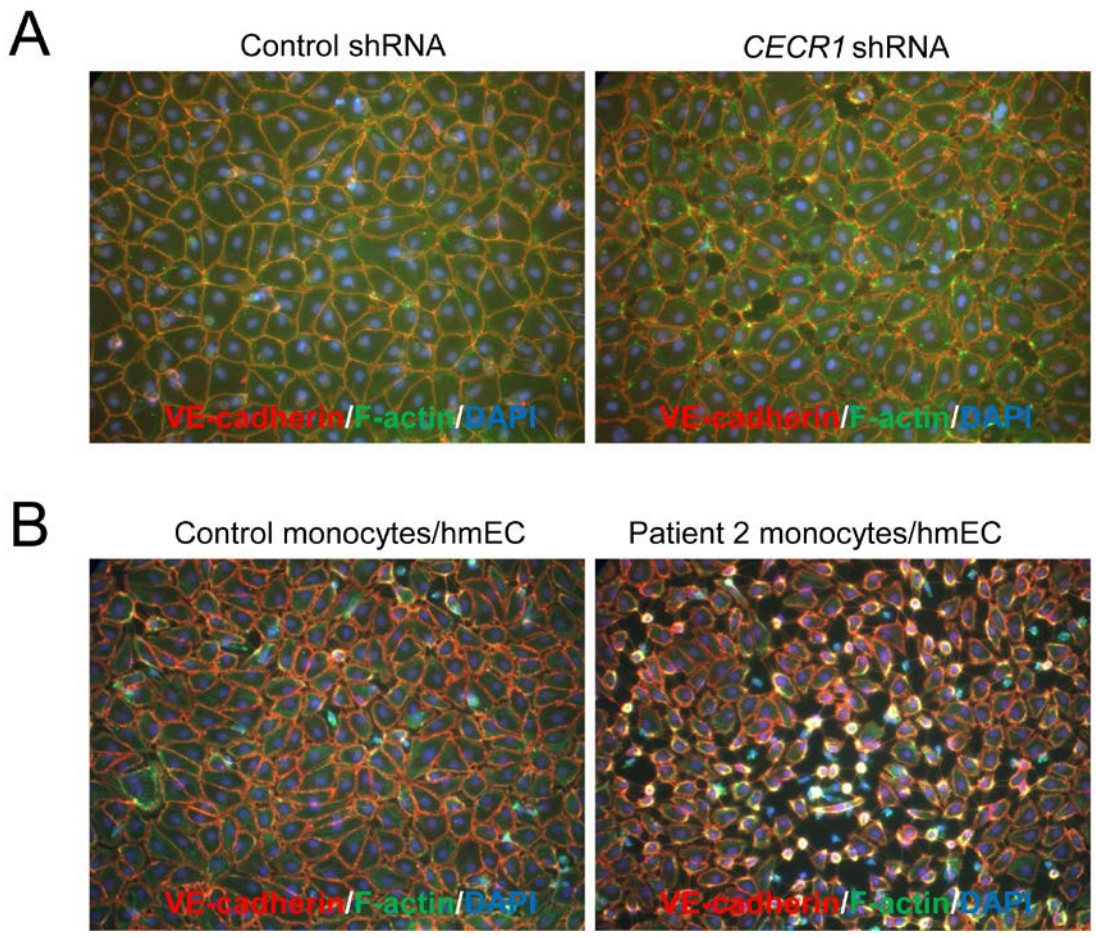

Figure S22. Effect of ADA2 Deficiency in U937 Myeloid Cells or Peripheral Blood Monocytes on their Interactions with Cultured Endothelial Cells

Human dermal microvascular endothelial cells (hmEC) were grown to confluence and were cocultured with human U937 myeloid cells for 24 hours (A) or monocytes from Patient 2 or a normal control donor for 3 days (B). Non-adherent cells were removed and the endothelial cell layers stained for the endothelial junction protein, VE-cadherin (red) and F-actin (green). Endothelial cell monolayers cultured with ADA2 knockdown (*CECR1* shRNA) U937 cells and with

monocytes isolated from Patient 2 show damaged, interrupted endothelial cell junctions compared to control shRNA U937 cells or healthy control monocytes. (Image magnification: 200X)

SUPPLEMENTARY TABLES

Table S1: Clinical Characteristics of NIH Patients with ADA2 Mutations and Recurrent Stroke

	Patient 1 (12yo)	Patient 2 (7yo)	Patient 3 (7yo)	Patient 4 (25yo)	Patient 5 (5yo)
Mutation	A109D/Y453C	G47A/Y453C	R169Q/deletion	G47A/H112Q	R169Q/Y453C
Fever	Yes	Yes	Yes	Yes	Yes
Stroke Onset	25 months	12 months	18 months	5 months	20 months
Birth Weight	3.12 kg	2.64 kg	4.68 kg	3.49 kg	3.86 kg
Ischemic Stroke Locations	R. thalamus, L. midbrain peduncle R internal capsule, basal ganglia, pons, anterior lumbar expansion (spinal cord)	R. thalamus and internal capsule	R. posterior thalamus, L. paramedian midbrain and pons	R. thalamus, R parietal cortex	L. posterior thalamus, L. posterior limb of internal capsule, R. caudate head, L. paramedian pons, L. posterior pons, R. deep white matter
Hemorrhagic Stroke Locations	None	L. cortical/ subcortical hemorrhage, R. caudate head and thalamic hematoma[1]	R. frontal-subdural, subarachnoid and frontal convexity hemorrhage, R. deep intraparenchymal hematoma[2]	R. deep intraparenchymal hematoma[3]	None
Intracranial MRA/Angiography Findings	MRA: normal Cerebral angiogram: normal	MRA: normal Cerebral angiogram: normal	MRA: normal	MRA: normal	MRA: normal Cerebral angiogram normal CT angiogram normal
Ophthalmologic	None observed	None observed	Orbital MRI: irregular enhancement in right medial rectus muscle	Central retinal artery occlusion	Left optic nerve atrophy
Dermatologic	Livedo racemosa	1) Livedo racemosa 2) Erythematous macules 3) Urticarial papules and plaques	1) Livedo racemosa 2) Urticarial papules and plaques	1) Livedo racemosa 2) Urticarial papules and plaques	Livedo racemosa

[1] ASA and warfarin, [2] ASA and clopidogrel, [3] warfarin only

* Age at most recent evaluation at NIH

Table S2. Additional Clinical Characteristics of NIH Patients with ADA2 Mutations and Recurrent Stroke

	Patient 1 (12yo)	Patient 2 (7yo)	Patient 3 (7yo)	Patient 4 (25yo)	Patient 5 (5yo)
Mutation	A109D/Y453C	G47A/Y453C	R169Q/deletion	G47A/H112Q	R169Q/Y453C
Gastrointestinal	Mild splenomegaly History of elevated hepatic transaminases	Hepatomegaly, splenomegaly, elevated hepatic transaminases, portal hypertension, grade 1 esophageal varices	Hepatomegaly, splenomegaly, chronic gastritis, elevated hepatic transaminases, normal portal pressures CT angiogram normal	Hepatomegaly, splenomegaly, elevated hepatic transaminases, celiac artery stenosis, portal hypertension	Hepatomegaly, splenomegaly, elevated hepatic transaminases
Liver biopsy	Not done	Changes suggestive of hepatoportal sclerosis (sinusoidal dilation and diffusely positive CD34 staining)	Mild portal inflammation and portal vein changes suggestive of hepatoportal sclerosis	Not done	Not done
Renal	Normal kidney size No hematuria No proteinuria	Nephromegaly No hematuria No proteinuria	Normal kidney size No hematuria No proteinuria	Normal kidney size No hematuria No proteinuria	Normal kidney size No hematuria Trace proteinuria
Hematologic	No abnormalities	Pancytopenia with lymphopenia	Leukopenia	Pancytopenia	Leukopenia
Bone Marrow Biopsy	Not done	Mildly hypocellular marrow with erythroid predominance and increased megakaryocytes B cell lymphopenia Absent iron stores	Normocellular marrow Active trilineage hematopoiesis Absent iron stores	Mildly hypocellular bone marrow Active trilineage hematopoiesis Absent iron stores	Not done
Additional	None	Bilateral carpal tunnel	Muscle MRI: enhancement consistent with myositis Muscle biopsy: perivascular inflammation with mononuclear cells without vasculitis	Cardiomyopathy Prolonged QT	Temporal artery biopsy: normal

Table S3. Stroke Histories of NIH ADA2 Deficient Patients

Age of Strokes	Stroke Location	Clinical Signs/Symptoms
Patient 1		
2 years 1 month	Pons Right internal capsule	Internuclear ophthalmoplegia
2 years 4 months	Medial thalamic lesion	Silent
2 years 4 months	Right basal ganglia Anterior thoracic-lumbar spinal cord infarct	Acute paraplegia Neurogenic bladder with urinary Incontinence
2 years 7 months	No MRI available	Aphasia Emotional lability
Patient 2		
12 months	No imaging done	Emesis Ataxia Transient left hemiparesis
17 months	Right medial thalamus	Ataxia Constricted right pupil
3 years 11 months	Right internal capsule	Fever Crying Left hemiparesis
4 years 4 months	No apparent new lesions	Left facial paralysis
4 years 9 months	Right temporal subdural hemorrhage	Altered mental status
4 years 10 months	Head of right caudate hemorrhage	Headache and neck pain
7 years 0 months	Left cerebral hemorrhage	Perception of tilted vision
Patient 3		
4 years 9 months	Right thalamus-hypothalamus	Right side ptosis Hemiparesis
4 years 11 months	Right occipital hemorrhage	Severe headache
4 years 11 months (2)	Left midbrain lacunar infarct	Increasing fatigue Decreased appetite Fevers
5 years 1 month	Large right frontal hemorrhage	Left hemiparesis
5 years 7 months	Left periacqueductal region Orbital MRI: irregular enhancement in right medial rectus muscle	Ophthalmoplegia Right ptosis
Patient 4		
5 months	Right lacunar Right thalamic Right parietal	Right side ptosis Left side hemiparesis
17 years	TIA	Right hand numbness Memory impairment
17 years (2)	TIA	Ataxia Dysphagia (Resolved)
25 years	Large left intraparenchymal hematoma	Right hemiparesis Severe expressive aphasia
Patient 5		
1 year 8 months	Left pons Right thalamus	Right side weakness Left III cranial nerve dysfunction
2 year 10 months	Rostral pons Caudal midbrain Right corona radiata	Decreased mental status Vomiting Left III cranial nerve dysfunction Truncal ataxia
3 years 2 months	Left thalamus Basal ganglia Internal capsule	Altered mental status Right side weakness
4 years 4 months	Right basal ganglia	Silent
4 years 6 months	Left medial temporal	Silent
4 years 7 months	Right putamen Right medial temporal lobe	Dysarthria Dysphagia
4 years 9 months	Left pons	Left facial weakness
5 years 1 month	Right centrum semiovale Left corona radiata Leptomeningeal enhancement	Silent

Table S4. Laboratory Values and Therapeutic History of NIH ADA2 Deficient Patients*

	Patient 1 (12yo)	Patient 2 (7yo)	Patient 3 (7yo)	Patient 4 (25 yo)	Patient 5 (5 yo)
Pre/post treatment ESR (mm/hr)	69/8	39/5	50/7	22/7	70/2
Pre/post treatment CRP	129/2.24	65/3.7	23/1.1	36.8/8.4	141/<5
WBC (K/uL)	18.3	11.2	10.6	18.9	15.5
ANC (K/uL)	10.7	3.6	1.3	9.1	N/A
ALC (K/uL)	5.73	N/A	8.2	8.9	N/A
Hemoglobin (g/dL)	10.3	9.3	10.6	N/A	11.6
Hematocrit (%)	30.7	31.5	31.9	33.7	36
Platelets (K/uL)	547	304	409	779	452
ALT (5-30 U/L)	24	55	49	123	46
AST (0-41 U/L)	29	61	47	86	31
IgG (572-1474 mg/dL)	992	1090 (on IVIG)	1210 (on IVIG)	577	417
IgA (34-305 mg/dL)	62	15	35	50	57
IgM (32-208 mg/dL)	28	<6	14	22	13
IgE (0-90 IU/mL)	Not tested	141	4.4	Not tested	Not tested
IgD (<10mg/dL)	1	<1	1	Not tested	Not tested
ANA (<1 EU)	4	2.7	Negative	Negative	Negative
Anti-dsDNA (0-30 IU/mL)	42	Negative	Negative	Negative	Negative
Anti-ENA(0-19 EU)	42 (anti-Sm) 23 (anti-RNP)	Negative	Negative	Negative	Negative
ANCA	Negative	Negative	Negative	Negative	Negative
Initial antiphospholipid antibody testing	Negative	Negative	Negative	Negative	Negative
Anticardiolipin IgG (0-12 GPL)	Negative	Negative	Negative	Negative	Negative
Anticardiolipin IgM (0-16 GPL)	Negative	Negative	Negative	Negative	Negative
PT (11.6-15.2 sec)/aPTT (25.3-37.3 sec)	Normal	Normal	Normal	Normal	Normal
Lupus anticoagulant	Negative	Positive	Positive	Positive	Positive
B2 glycoprotein antibodies	Not tested	Negative	Negative	Negative	Negative
Protein C (72-149%)	Normal	Normal	Normal	Normal	Normal
Protein S (64-131%)	Normal	Normal	Normal	Normal	Normal
Prothrombin 20210 mutation analysis	Negative	Negative	Not tested	Negative	Negative
Factor V Leiden muatation analysis	Negative	Negative	Negative	Negative	Negative
Homocysteine	Normal	Normal	Normal	Normal	Normal
MTHFR	Not tested	Not tested	Heterozygous	Heterozygous	Not tested
Medications (current and prior)					
Steroids	Yes	Yes	Yes	Yes	Yes
Cyclophosphamide	Yes	Yes	Yes	Yes	Yes
Anakinra	Yes	Yes	Yes	Yes	Yes
IVIG	Yes	Yes	Yes	Yes	Yes
Mycophenolate	No	Yes	No	Yes	No
Etanercept (initiated 6/13)	Yes	Yes	Yes	Yes	Yes

***Blood counts were taken at initial clinical presentation and immunoglobulins were drawn at initial NIH presentation. Liver function tests and autoantibodies were the most recent values obtained at the NIH, except for the initial antiphospholipid antibodies. The coagulation studies were performed prior to presentation to the NIH, over the course of the patients' illness.**

Table S5. Clinical Spectrum of Non-NIH Patients with ADA2 Mutations

	Patient 6 (15yo)	Patient 7 (10yo)	Patient 8 (15yo)	Patient 9 (22yo)
Mutation	M1T/I93T	G47R/G47R	G47R/G47R	G47R/G47R
Fever	Yes	Yes	Yes	Yes
Neurologic	Ischemic strokes at 18 months and 6 years	Ischemic stroke at 3.5 years	Ischemic stroke at 4 years	Borderline intelligence
CNS Imaging	MRI: left thalamic and basal ganglia lesions MR angio: normal Carotid and vertebral arteriography: normal	MRI: lesions of pons and just medial to right crus cerebri	MR angio: left cerebral cortical and subcortical lesions Decreased caliber of right posterior cerebral artery	MRI: Nodular small lesions with contrast enhancement of the right caudate nucleus
Ophthalmologic	None	Strabismus CN III palsy	None	Strabismus
Dermatologic	Non-Langerhans cell histiocytosis Generalized eruptive histiocytoma	Erythema nodosum Livedo racemosa	Erythema nodosum Livedo racemosa	Livedo racemosa Erythematous macules Necrotic ulcers on extremities and ears
Hematologic	Evans syndrome	No abnormalities	Macrophage activation syndrome	Paraaortic and inuguinal lymphadenopathy Leukopenia
Bone Marrow Biopsy	Normal trilineage hematopoiesis Prominent reactive lymphoid follicles in the interstitium Few small non-necrotizing granulomata	Not done	Not done	Idiopathic myelofibrosis Lymphohistiocytic aggregates
Gastrointestinal	Hepatomegaly Splenomegaly Portal hypertension Spleno-renal shunt Hepatopulmonary syndrome Liver transplant Abdominal MRA: normal	N/A	Bowel perforation at age 8 requiring resection and ileostomy	Hepatomegaly Splenomegaly History of ascites AA amyloid via intestinal biopsy Diarrhea Pancreatitis
Liver biopsy	Nodular regenerative hyperplasia	Not done	Not done	Not done
Renal	Arterial hypertension post-spleno-renal shunt	Normal	Normal	AA amyloidosis 7gm protein/24 hours
Autoantibodies	Antiphospholipid antibodies negative ANA negative ANCA negative	Antiphospholipid antibodies negative ANA negative ANCA negative	ANA negative ANCA negative	Antiphospholipid antibodies negative ANA: 1:320 P and C ANCA negative Lupus anticoagulant positive
Other	None	Sibling of Patient 8	Sibling of Patient 7	Product of consanguineous relationship Growth retardation
Steroids	Yes	Yes	Yes	Yes
Cyclophosphamide	No	No	Yes	Yes
Rituximab	Yes	No	No	No
Anakinra	No	No	No	No
Etanercept	No	No	Yes	No
Tocilizumab	No	No	No	Yes

Table S6. Pathogenicity of *CECR1* Mutations Identified in 9 Affected Cases

Mutations	dbSNP	1000 Genomes MAF	NHLBI 6500 exomes MAF	ClinSeq 801 exomes MAF	SIFT and PolyPhen2 prediction
28kb deletion	/	/	/	/	/
p.Met1Thr	/	/	/	/	Damaging
p.Gly47Arg	/	/	/	/	Damaging
p.Gly47Ala	rs200930463	0.001	/	0.0005	Damaging
p.Ile93Thr	/	/	/	/	Damaging
p.Ala109Asp	/	/	/	/	Damaging
p.His112Gln	/	/	/	/	Damaging
p.Arg169Gln	rs77563738	0.0005	0.000538	/	Damaging
p.Tyr453Cys	/	/	0.000154	/	Damaging

Missense variants are predicted to have a damaging effect on protein function by PolyPhen2 (Polymorphism Phenotyping, version 2) and SIFT (Sorts Intolerant from Tolerant Substitutions). MAF, minor allele frequency.

Table S7. Plasma ADA2 and ADA1 Enzymatic Activity (mU/mL)

Individuals		ADA2	ADA1
Patients (Mean±SD)		1.0±0.5	4.4±2.7
	Patient2 (G47A/Y453C)	1.4	2.8
	Patient3 (R169Q/deletion)	0.6	8.4
	Patient4 (G47A/H112Q)	1.4	3.6
	Patient5 (R169Q/Y453C)	0.5	2.7
Parents (Mean±SD)		4.9±0.4	3.2±0.9
	Mother4 (H112Q/wt)	5.3	3.6
	Father5 (Y453C/wt)	4.7	3.7
	Mother5 (R169Q/wt)	4.6	2.1
Controls (Mean±SD)		14.0±6.1	4.4±2.4
	Pooled plasma	15.2	2.9
	Control1	16.2	5.0
	Control2	21.3	6.8
	Control3	17.6	7.5
	Control4	8.6	1.5
	Control5	4.8	2.8

For ADA2 enzymatic activity, the P value is significant between patients and parents ($P<0.001$), and significant between patients and controls ($P=0.003$).

Table S8. *CECR1* Mutations in ADA2 Deficient Patients

Chr	Position	Reference	Variant	Variant Function	cDNA Change	Amino Acid Change	Position
chr22	17695127-17723376	/	/	Genomic deletion	/	/	5' UTR and exon1
chr22	17690566	A	G	nonsynonymous SNV	NM_017424.2: c.T2C	p.Met1Thr	exon2
chr22	17690429	C	T	nonsynonymous SNV	NM_017424.2: c.G139A	p.Gly47Arg	exon2
chr22	17690428	C	G	nonsynonymous SNV	NM_017424.2: c.G140C	p.Gly47Ala	exon2
chr22	17690290	A	G	nonsynonymous SNV	NM_017424.2: c.T278C	p.Ile93Thr	exon2
chr22	17688177	G	T	nonsynonymous SNV	NM_017424.2: c.C326A	p.Ala109Asp	exon3
chr22	17688167	G	C	nonsynonymous SNV	NM_017424.2: c.C336G	p.His112Gln	exon3
chr22	17687997	C	T	nonsynonymous SNV	NM_017424.2: c.G506A	p.Arg169Gln	exon3
chr22	17662794	T	C	nonsynonymous SNV	NM_017424.2: c.A1358G	p.Tyr453Cys	exon9

SUPPLEMENTARY REFERENCES

1. Zavialov AV, Yu X, Spillmann D, Lauvau G, Zavialov AV. Structural basis for the growth factor activity of human adenosine deaminase ADA2. J Biol Chem 2010;285:12367-77.
2. Kohn DB, Kantoff PW, Eglitis MA, et al. Retroviral-mediated gene transfer into mammalian cells. Blood Cells 1987;13:285-98.
3. Arredondo-Vega FX, Kurtzberg J, Chaffee S, et al. Paradoxical expression of adenosine deaminase in T cells cultured from a patient with adenosine deaminase deficiency and combine immunodeficiency. J Clin Invest 1990;86:444-52.
4. Hershfield MS, Fetter JE, Small WC, et al. Effects of mutational loss of adenosine kinase and deoxycytidine kinase on deoxyATP accumulation and deoxyadenosine toxicity in cultured CEM human T-lymphoblastoid cells. J Biol Chem 1982;257:6380-6.
5. Kotlarz D, Zietara N, Uzel G, et al. Loss-of-function mutations in the IL-21 receptor gene cause a primary immunodeficiency syndrome. J Exp Med 2013;210:433-43.
6. Moir S, Buckner CM, Ho J, et al. B cells in early and chronic HIV infection: evidence for preservation of immune function associated with early initiation of antiretroviral therapy. Blood 2010;116:5571-9.
7. Westerfield M. The Zebrafish Book: A Guide for the Laboratory Use of Zebrafish (*Danio rerio*). 4th ed: University of Oregon Press; 2000.
8. Thisse C, Thisse B. High-resolution in situ hybridization to whole-mount zebrafish embryos. Nat Protoc 2008;3:59-69.
9. Detrich HW, 3rd, Kieran MW, Chan FY, et al. Intraembryonic hematopoietic cell migration during vertebrate development. Proc Natl Acad Sci U S A 1995;92:10713-7.
10. Lawson ND, Weinstein BM. In vivo imaging of embryonic vascular development using transgenic zebrafish. Dev Biol 2002;248:307-18.
11. Traver D, Paw BH, Poss KD, Penberthy WT, Lin S, Zon LI. Transplantation and in vivo imaging of multilineage engraftment in zebrafish bloodless mutants. Nat Immunol 2003;4:1238-46.
12. Renshaw SA, Loynes CA, Trushell DM, Elworthy S, Ingham PW, Whyte MK. A transgenic zebrafish model of neutrophilic inflammation. Blood 2006;108:3976-8.
13. Varshney GK, Lu J, Gildea DE, et al. A large-scale zebrafish gene knockout resource for the genome-wide study of gene function. Genome Res 2013;23:727-35.